2 GCA-TR-71-1-N

MASS SPECTROMETER FOR D-REGION STUDIES
PART 1: LABORATORY TESTS

R. F. K. Herzog

Get DRA

GCA CORPORATION
Bedford, Massachusetts

FINAL REPORT
PHASE I
CONTRACT NO. NASW-1314

PREPARED FOR
NATIONAL AERONAUTICS AND SPACE ADMINISTRATION
HEADQUARTERS
WASHINGTON, D. C.

February 1971

GCA-TR-71-1-N

MASS SPECTROMETER FOR D-REGION STUDIES

PART 1: LABORATORY TESTS

R. F. K. Herzog

GCA CORPORATION
GCA TECHNOLOGY DIVISION
Bedford, Massachusetts

FINAL REPORT
PHASE I

Contract No. NASW-1314

February 1971

Prepared for

NATIONAL AERONAUTICS AND SPACE ADMINISTRATION
HEADQUARTERS
WASHINGTON, D.C.

TABLE OF CONTENTS

LIST OF ILLUSTRATIONS

LIST OF ILLUSTRATIONS (Continued)

LIST OF TABLES

MASS SPECTROMETER FOR D-REGION STUDIES

by
R. F. K. Herzog
GCA Corporation, GCA Technology Division, Bedford, Massachusetts

SUMMARY

Analysis of the ion composition in the D-region is much more difficult than in the E-region since the pressure in the D-region is so high that a pump is required to keep the pressure in the mass spectrometer in the 10^{-4} torr range. In addition to this, the ion densities in the D-region are lower, and the neutral densities much higher. The ion composition of the D-region has been measured in the past with a quadrupole type mass spectrometer combined with a zeolite cryogenic pump. It is the purpose of this study to determine whether the combination of a monopole mass spectrometer with a titanium getter pump has advantages over the previously used method.

SECTION I

INTRODUCTION

The performance of monopole mass spectrometers has been thoroughly investigated both theoretically and experimentally. Compared with the quadrupole mass spectrometer, it requires much less power to operate which is most important if heavy molecules have to be analyzed. The mechanical adjustments are less critical and the power supply is much simpler. These properties are of great value for space applications. Counting technique of single ions has been used to obtain negative ion spectra. A novel sweep method permits the extension of the regular mass range to very high mass numbers at reduced resolution without increase of the power consumption.

The pumping capacity of a titanium getter pump has been investigated. For good performance it is essential that the active titanium layer is deposited under ultra-high vacuum conditions. Nitrogen is pumped faster, in larger quantities and more completely if the active getter is heated to about 200°C. The laboratory tests have indicated that the pumping capacity of the titanium getter pump is quite adequate to permit analysis of the ion composition in the D-region with a monopole mass spectrometer.

A. Monopole Mass Spectrometer

The main objective of the work under this contract was to evaluate the performance of the monopole mass spectrometer. A large amount of practical experience has been gained with two different monopole mass spectrometers which have been used to obtain more than 1000 spectra. It has been found that the monopole mass spectrometer is a very reliable and extremely useful instrument if used in an ultra-high-vacuum system, although the requirements for cleanliness (especially freedom from oil vapors from the diffusion pump) are more severe with this instrument than with others. This is not a serious drawback for those applications where the instrument can be evacuated with ion pumps or getter pumps. Compared with the quadrupole mass spectrometer, it has a number of important advantages which are of special value for space applications. The RF power supply is much simpler since the DC to AC voltage ratio is not critical. Quadrupole mass spectrometers require a well-balanced, push-pull output whereas for monopole mass spectrometers a single-pole output is sufficient. The voltages which are required to cover a certain mass range are much lower for the monopole instrument. This feature is very valuable if either a very wide mass range should be covered (as is the case for this study of the ions in the D-region), or for other space applications where the instrument must be operated continuously with very limited power. A special type of scanning has been successfully utilized with this instrument which permits extending the mass range well above mass 400 without any additional power requirements. The low mass range (for instance, mass 1 to 50) is scanned in the usual manner with increasing resolution. The extended mass range (for instance, mass 50 to 500) is scanned with gradually reduced resolution. This method of scanning permits the detection of any heavier masses present without the need of extending the scanning time to such large values that are no longer compatible with a fast moving rocket.

It was suspected that the overall sensitivity of the monopole instrument would be much lower than that of the quadrupole instrument since ions which enter the monopole field during the wrong phase of the RF field would be deflected towards the V electrode and lost. However, it was possible to reduce this disadvantage by a slight deflection of the incoming ion beam. A 10-fold increase in sensitivity has been obtained. After a large number of systematic experiments it was found that the highest sensitivity for a peak width of one mass unit can be obtained with fairly wide entrance and exit apertures and with any chosen value of the DC to AC voltage ratio if the ion energy is kept below a certain value which is a function of this ratio. Under these optimum operating conditions the sensitivity of the monopole mass spectrometer is about equal to the quadrupole mass spectrometer. The main advantage of the monopole mass spectrometer is the fact that the adjustments of all operating voltages is much less critical, which permits scanning over a very wide mass range (for instance, mass 1 to 500) without need to change the frequency. Higher reliability for space applications must be expected since extreme space environment conditions may cause a wider variation in the operating voltages which will not affect the performance of the instrument.

Experiments have proved that the analysis of negative ions is also possible with the monopole mass spectrometer. Secondary electrons released from points of impact of the ions did not increase the general background noise level of the mass spectra. The main difficulty in detecting negative ions comes from the fact that the anode of the electron multiplier is at high voltage (approximately 3000 volts), and that extremely small currents have to be measured there. This difficulty has been resolved by a pulse-counting technique whereby the pulse amplifier input is kept near ground potential and is coupled capacitively to the multiplier anode.

The pulse-counting technique has been improved and tested and has shown very promising results. Each ion that arrives on the first dynode of the electron multiplier triggers an artificial pulse of constant length and height. This reduces significantly the effect of variations of the multiplier gain, either due to changes in the operating voltage or to changes in the surface conditions of the dynodes. Therefore, a higher accuracy for the measurements must be expected.

Several methods have been tested to display the normalized pulses. A pulse rate meter capable of detecting single pulses with either linear or semi-logarithmic display has been developed. The method permits much faster scanning over the whole mass spectrum, since the scanning speed is no longer limited by the relatively large time constant of an electrometer in the 10^{-13} amperes range. Now the scanning speed is limited only by the fundamental statistical variations due to the limited number of ions collected in one mass peak.

A second method to record a mass spectrum has also been tested successfully. In this case the integral of the mass spectrum has been displayed. Therefore, each peak in a normal mass spectrum corresponds to a step in a staircase-type spectrum. This kind of display of a mass spectrum is especially valuable for deep space probes since the telemetry requirements for the transmission of a staircase-type curve are much less demanding than for a spectrum consisting of a large number of very narrow and sharp peaks. Another advantage of this integrating method comes from the fact that all the ions within a mass peak are added together which reduces the statistical error of the measurement. The display can be either such that the height of each step is a linear function of the intensity of the mass peak or a semi-logarithmic function. The first one is useful for the measurement of the mean peaks if no great variations of intensity are expected. The latter one covers a very wide intensity range of the mass peaks with the emphasis on the small peaks. These sophisticated counting techniques require a careful balance of scanning speed, single-pulse duration and integrating time in relation to the signal strengths and the overall objective of the special mission. It has been demonstrated that the new counting techniques are quite capable of pushing the sensitivity and the scanning speed to the very limit where every single ion is recorded.

B. Titanium Getter Pumps

The second objective of the work under this contract was a test of the performance of a titanium getter pump. The main advantage of such a pump compared with a sorption pump is that it does not require liquid nitrogen for cooling. Therefore, condensation of water and ice on some spots of the rocket cannot occur, and contamination of the ambient atmosphere with water vapor released from the rocket will be greatly reduced.

It has been expected (and later experiments have confirmed this) that the performance of the titanium getter pump depends largely on the method by which the titanium film has been prepared. In the usual sublimation pump the pressure increases considerably due to out-gasing during the evaporation process of the titanium. This gas, mainly hydrogen from the decomposition of titanium hydride, is reabsorbed on the newly-formed titanium layer on the walls. Therefore, a considerably part of the newly-formed titanium layer is inactive for further absorption. In order to prevent this from happening, it is necessary to produce the titanium film on the wall during the time of the bake-out of the system. At this temperature titanium hydride will not be formed. A well-trapped diffusion pump system is necessary to remove the large amount of hydrogen and other contaminants, especially methane.

An Orb Ion Pump has been used to produce the titanium getter film. The measurements have been performed either with a 6" NRC Orb Ion Pump or with a smaller Orb Ion Pump built under this contract. The general experience with the pump is very good. A pressure in the 10^{-9} range can easily be obtained and maintained permanently. No contamination of the mass spectrometer has been observed, and excellent reproducibility of the measurements has been achieved. The pumping speed for nitrogen, oxygen, argon, and air was approximately in agreement with the values supplied by NRC. In the course of the investigation some measurements have been made with krypton and xenon, with osmium tetra-oxide, with acetone, with perfluorodymethylcyclohexane, and with sulphur hexafluoride. All those materials have been pumped fairly well. The only gas which is pumped extremely poorly is water vapor. The background gas in the running pump consists mainly of methane, CO, H_2O, H_2, and H. If the pump is switched off, the titanium layer on the wall releases argon which has been previously pumped. A short time after shut-down the gas in the pump consists practically entirely out of argon. However, the total pressure did not increase above the 10^{-6} range, and the argon did not interfere with the operation of the mass spectrometer. If the pump is switched on again, the argon is removed rapidly even if the pump current is reduced to as little as 1 milliampere. In this case the pumping action is caused only by ionization since the power consumption of the pump is so low that no new titanium will be sublimated. Most of the measurements of the monopole mass spectrometer have been performed with air at a constant

pressure of 2×10^{-8} torr which was constantly bled into the system. A reduced pump current of 20 milliamperes was sufficient to keep the system at this low pressure. The pump was operated under these conditions for about half a year without any sign of performance reduction.

Most work was done to study the absorption characteristic of a fresh titanium layer prepared under high vacuum conditions. After this layer has been formed, all the voltages of the Orb Ion Pump have been switched off. An increasing amount of air has been introduced into the system, and mass spectra of the residual gas have been recorded. As expected, argon has not been absorbed at all, and the partial pressure of argon increased as if there were no titanium layer on the wall. Oxygen is absorbed very rapidly and is permanently removed from the system.

An unsuspected behavior has been found with nitrogen. If the wall of the titanium pump is kept at room temperature, only about 98 percent of the introduced nitrogen has been absorbed. The rest of 1-2 percent remains in the gas phase, despite the fact that the titanium layer is still unsaturated. This percentage increased when the saturation of the titanium layer was approached. However, when the almost saturated pump was heated to approximately $200^{\circ}C$, no release of nitrogen was observed. On the contrary, the residual nitrogen which had not been pumped before, was quickly absorbed. The hot titanium film absorbs nitrogen much faster and more completely and permanently. The total amount of nitrogen which can be absorbed before saturation occurs is considerably higher for a hot titanium layer. It has been found that this amount corresponds to approximately 10 monolayers. This means that the surface of the titanium layer is either porous or very rough and has a much larger effective surface area than the geometrical area of the pump wall. It is also possible that nitrogen diffuses into deeper layers of the titanium film, a process which would be enhanced by higher temperatures. If a very large amount of air is suddenly introduced into the hot titanium getter pump, the residual gas is almost entirely argon and the argon partial pressure increases into the micron range before any signs of saturation for nitrogen are observed.

In conclusion, both the monopole mass spectrometer as well as the titanium getter pump are very well suited for the intended purpose of measuring the ionic composition of the D-region. Greater simplicity of the system, improved convenience and reliability of operation, and reduced contamination of the ambient atmosphere are some of the valuable features of this sytem. Therefore, a flight instrument has been designed, tested and delivered. It has been described in Part II of the Final Report of Contract NASw-1314.

SECTION II

PERFORMANCE CHARACTERISTICS OF A MONOPOLE MASS SPECTROMETER WITH TRANSVERSE MAGNETIC FIELD

A. Introduction

Since its invention approximately 7 years ago by Ulf von Zahn (Ref. 1) the monopole mass spectrometer has become an extremely valuable analytical tool. Although its behavior is in general quite similar to the longer known quadrupole mass spectrometer, several specific differences exist which have to be understood and considered in order to utilize the full capabilities of this instrument. It will be the purpose of this paper to study these differences theoretically and to compare the results with the actual performance of a monopole mass spectrometer. The theory of the monopole mass spectrometer is hampered by the fact that the ion orbits are Mathieu functions which are not sufficiently tabulated and that the combined effect of a large number of different parameters has to be considered. Some selected orbits have been studied with the aid of computers by R.F. Lever (Ref. 2), and more recently by P.H. Dawson and N.R. Whetten (Ref. 3). Despite all this effort, the full understanding of the basic behavior of ions in the monopole field is still hidden behind the complex mathematical theory.

The theory which will be used here is based on Brubaker's (Ref. 4) approximations for a quadrupole mass spectrometer, since they provide a better insight into the behavior of the instrument than the accurate theory. However, the conditions for ion transmission are more stringent in a monopole than in a quadrupole instrument since ions can no longer cross the symmetry planes between the quadrupole rods. The effect of a transverse magnetic field, which produces a large increase of the sensitivity of the monopole mass spectrometer (Ref. 5), can be easily studied with this method.

B. Motion of Ions in the Monopole Field

The orientation of the coordinate system and the direction of the magnetic field in relation to the V- and rod-electrode and the triangular entrance and exit apertures are shown in Figure 1. The characteristic feature of the quadrupole and monopole field is that the electric field strength should be proportional to the distance from the axis. This would require hyperbolically shaped electrodes which are difficult to machine. In general, round electrodes with a diameter $D = 2.32 \times r_0$ are used to produce a field which is close to the desired one if the beam does not come near to the electrodes. Brubaker (Ref. 6) has shown recently that this approximation causes an appreciable loss of resolution or sensitivity in a quadrupole instrument. It can be expected that also a monopole instrument could be improved by replacing the rod with a hyperbolically shaped cylinder.

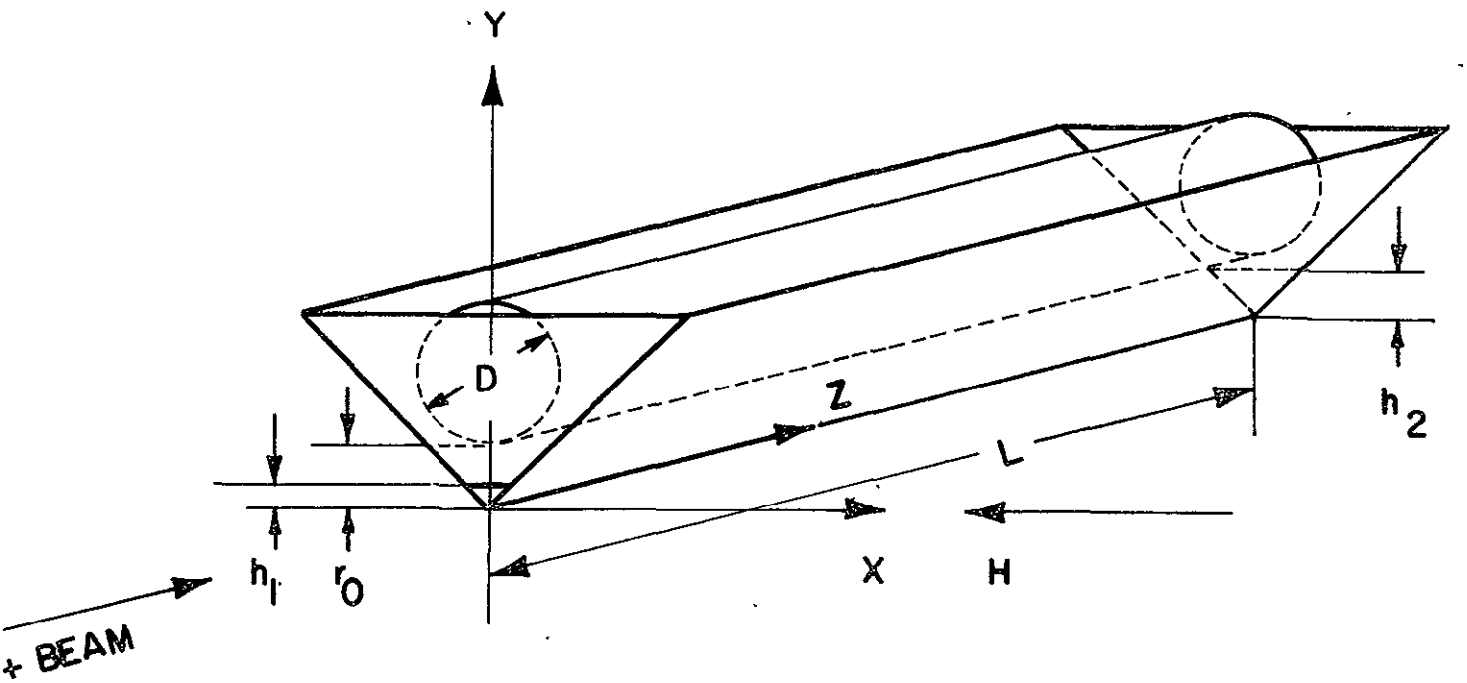

Figure 1. Monopole structure coordinate system.

The following table lists all parameters which will be used in the calculations.

Table 1

ABBREVIATIONS

U	Absolute value of the DC voltage on rod, measured in volts. U is a negative for positive ions.
V	Amplitude of AC voltage on rod = 1/2 of peak to peak value.
$R=\|U\|/V$	Voltage ratio, usually kept constant and smaller than 0.167.
$\nu=1/\tau$	Frequency of the AC voltage in cycles per second.
$\omega=2\pi\nu$	
E	Acceleration voltage of ions in volts.
H	Magnetic field strength in Oerstead (Gauss).
r_o	Field radius in cm = distance of rod surface to axis.
L	Length of field in cm = distance from entrance to exit aperture.
$\alpha_o=r_o/L$	Form factor of field.
h_1, h_2	Height of triangular entrance and exit aperture in cm.
a,q,β,μ	Characteristic parameters of the Mathieu functions.
$s = 1/\beta$	Number of RF cycles required for one half major oscillation in the y-direction.
$N=\nu L/v$	Number of RF cycles required for an ion to travel through the field of length L.

e = 4.8×10^{-10} est. units = charge of singly charged ions

M = Mass number

m_1 = 1.66×10^{-24} g

m = $M \times m_1$ mass of ion in grams

v = Ion velocity in cm/sec

ϕ_o = Phase of the AC field at the time when the ion enters the field

P = Power consumption in watt

The equations of motion in the x- and y-direction are given by Equations (1) and (2):

$$m \ddot{x} = -2\, e \left[U/300 + (V/300) \cos (\phi_o + \omega t)\right] (x/r_o^2) \qquad (1)$$

$$m \ddot{y} = +2\, e \left[U/300 + (V/300) \cos (\phi_o + \omega t)\right] (y/r_o^2) + ev\, H/C \qquad (2)$$

If the fringe fields at the entrance- and exit-aperture are neglected the axial velocity v is the same inside and outside the field and given by:

$$v = \sqrt{eE/(150\, Mm_1)} \qquad (3)$$

We introduce the instrument constant U^* which is only a function of the instrument parameters r_o and ω:

$$U^* = 300\, (\omega\, r_o)^2\, m_1/e \text{ volts} \qquad (4)$$

The Equations of motion (1) and (2) can be transformed into Equations (5) and (6):

$$\ddot{x} = -\,(a + 2q \cos (\phi_o + \omega t))\, \omega^2\, x/4 \qquad (5)$$

$$\ddot{y} = + (a + 2q \cos (\phi_o + \omega t))\ \omega^2\ y/4 + (e/m)^{3/2}\ \sqrt{E/150}\ (H/c) \quad (6)$$

if the following substitutions are made:

$$a = 8\ (U/U^*)/M \quad (7)$$

$$q = 4\ (V/U^*)/M \quad (8)$$

The solutions of Equation (5) are Mathieu functions if t is replaced by:

$$2\xi = \phi_o + \omega t \quad (9)$$

The solution of the inhomogeneous Equation (6) can also be expressed by Mathieu functions and their integrals (see McLachlan) (Ref. 7). However, the results of these exact calculations are complicated and not easily understood. Therefore, the effect of the magnetic field will be better described by an approximation method.

The Mathieu functions are either stable or unstable depending upon the value of the parameters q and a. If the function is unstable the amplitude increases progressively with time. If the function is stable the amplitude does not exceed a certain limit and becomes periodically rather small. It is a wide-spread belief that only those ions can pass the filter which have orbits described by stable Mathieu functions. This is only true if the length of the filter or the frequency ν would be infinite or the ion velocity v be zero. For real filters of finite lengths it is quite possible that also ions whose orbits are unstable Mathieu functions can pass the filter. In practice one tries to operate the monopole filter with the lowest frequency and highest ion energy compatible with adequate resolution in order to obtain high sensitivity and low RF power consumption. For practical reasons, one also uses the shortest filter possible. All these choices favor the transmission of ions with "unstable" orbits.

It is obvious that all ions regardless of mass can pass the filter if they travel exactly on the axis of the instrument where the electric field

is zero. Even for a very narrow beam around the axis the electric field is neglibibly small. This beam can be fairly large if the ion energy is so high that only a few cycles of the RF field are needed for an ion to pass the filter. Therefore, the consideration of stable as well as unstable solutions is required to describe adequately the behavior of the mass filters. The effect of the unstable orbits is quite noticeable around the hydrogen peak. First, because hydrogen ions have the fastest velocity in the filter and require the smallest number of RF-cycles to pass the field. Second, the voltages applied to the rod are very small which permits heavier ions to pass the filter. This causes a considerable background around the hydrogen peaks especially below mass number 1.

The maximum value of q is determined by the stability requirement in the x-direction. Since monopole instruments are normally operated far below this limit, the oscillations in the x-direction have a small amplitude and little effect on the performance of the instrument. Therefore, this paper will deal only with the oscillation in the y-direction which are of prime importance for the understanding of the instrument. The oscillations in the x-direction have been adequately treated in the referred papers.

C. Approximate Solutions of the Equation of Motion

The most important and difficult part of the derivation of a useful approximate solution is the recognition of which terms can be neglected without any serious effects on the results.

It will be shown later that "a" is always much smaller than q. Therefore, for the first approximation, we neglect "a" in Equation (6) and assume that the magnetic field is zero. In this case Equation (6) is simplified to

$$\ddot{y} = y\ 0.5\ \omega^2\ q \cos\ (\phi_o + \omega t) \qquad (10)$$

and describes the effect of the AC field alone.

Small oscillations with the frequency ν in a homogeneous AC field.- The obstacle for a simple integration of Equation (10) is the variable y on the right side which is characteristic for the inhomogeneous monopole field. However, we will see later that the amplitude of the oscillations of an ion in a monopole field under normal operating conditions is always much smaller than the average distance $\bar{y}$ from the axis of the instrument. This permits, for the first approximation, the replacement of the inhomogeneous field by a homogeneous field with the same field strength in the center of the oscillation. To do this we replace the variable y on the right side of Equation (10) by the constant $\bar{y}$ which represents the average value of y during one cycle of the AC field.

This simplification is permitted only if y never becomes zero. Therefore, the following calculations are not applicable for any case where the beam crosses the axis. The distance from the axis can be rather small, as long as it is larger than the change of this distance during one cycle of the oscillation. A monopole filter is usually operated with an ion source that produces a well collimated narrow beam parallel to the axis. During one cycle of the field the ions move along only a small fraction of the field length. Therefore the change in their distance from the axis is really very small. The immediate vicinity of the axis can be excluded by the shape of the entrance aperture. However, this is not really necessary since even for the generally used triangular entrance aperture the contribution of ions that enter near the axis, is negligibly small.

A more accurate calculation which includes crossing of the axis is possible if one assumes $\bar{y}$ to be a linear function of time. However, the results are much more complicated and contain twice as many terms. Since they do not contribute much to the understanding of the normal operation of the monopole filter they will be omitted here. Therefore, the factor

$$A = \bar{y}\ 0.5\ \omega^2\ q$$

becomes a constant and Equation (10)

$$\ddot{y} = A \cos\ (\phi_o + \omega t) \qquad (11)$$

represents a forced oscillation. This equation can be easily integrated. One obtains

$$\dot{y} = (A/\omega) \sin\ (\phi_o + \omega t) + c$$

$$y = -(A/\omega^2) \cos(\phi_o + \omega t)\ + ct + d$$

The integration constants c and d are determined by the initial conditions. Let us assume an ion enters the field at the time t = 0 and at the point y_o and in the direction α against the axis of the instrument. One obtains

$$\alpha v = \bar{y}\ 0.5\ \omega\ q \sin\ \phi_o + c \qquad \text{and}$$

$$y_o = -\bar{y}\ 0.5\ q \cos\ \phi_o + d$$

which results in

$$y = -\bar{y}\ 0.5\ q \cos(\phi_o + \omega t) + (\alpha v - \bar{y}\ 0.5\ \omega\ q \sin \phi_o)t + y_o + \bar{y}\ 0.5\ q \cos \phi_o \quad (12)$$

One can easily verify that this equation fulfills both, the initial conditions and the differential equation.

Since the average value of $\cos(\phi_o + \omega t)$ over one full cycle is zero, the average value of y for the time t = 0 becomes

$$\bar{y} = y_o + \bar{y}\ 0.5\ q \cos \phi_o$$

and shall be called $\bar{y}_o$. This results in

$$\bar{y}_o = y_o/(1 - 0.5\ q \cos \phi_o) \quad (13)$$

This means that the centerline $\bar{y}_o$ of the oscillations normally does not go through the point of entry y_o.

In addition, the average y-velocity in the field is normally also different from the y-velocity αv outside the field and given by

$$\dot{\bar{y}}_o = \alpha v - y_o\ 0.5\ \alpha\ q \sin \phi_o/(1 - 0.5\ q \cos \phi_o) \quad (14)$$

It should be noticed that for $\phi_o = 0$ and π the lateral displacement is a maximum and the angular deflection is zero. For $\phi_o = \pi/2$ and $3\pi/2$ the lateral displacement is zero and the angular deflection a maximum. There exists no phase angle where both displacement and deflection disappear simultaneously. Therefore, even the best collimated beam is spread out by the momentum transfer during the first cycle of the AC field. This is demonstrated in Figure 2 which shows four typical orbits in a homogeneous field.

Using $\bar{y}_o$ and $\dot{\bar{y}}_o$, Equation (12) can be written in the form

$$y = \bar{y}_o + \dot{\bar{y}}_o\ t - \bar{y}_o\ 0.5\ q \cos(\phi_o + \omega t) \quad (15)$$

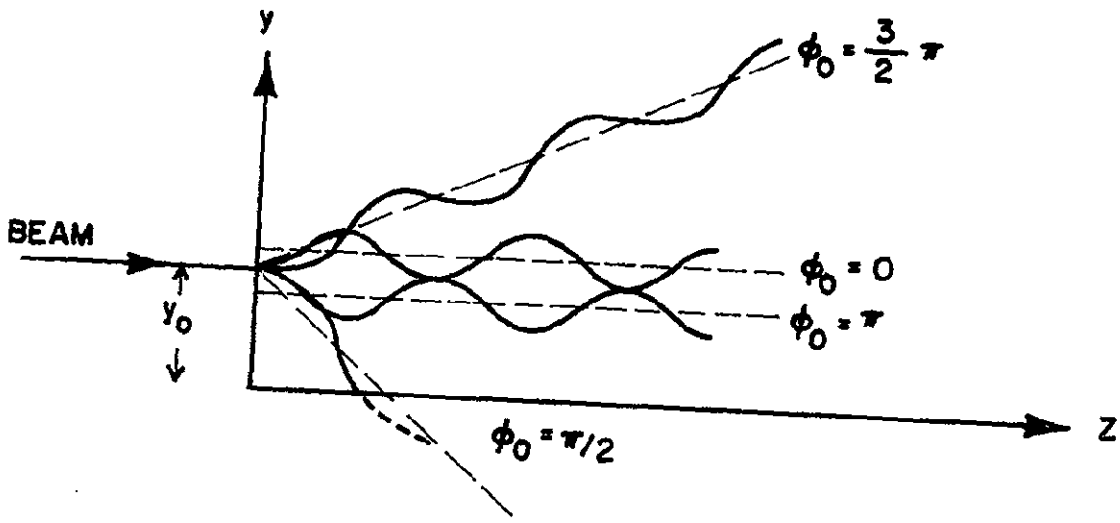

Figure 2. Impulse transfer during the first RF cycle.

This describes an oscillation with the frequency ν and the constant amplitude $\bar{y}_o$ 0.5 q about the straight line $\bar{y}_o + \dot{\bar{y}}_o t$. Monopole filters are normally operated with q values between 0.3 and 0.7. Therefore, the amplitude of the oscillations is really small, about 1/4 of the distance $\bar{y}_o$ to the axis. The replacement of the inhomogeneous field by a homogeneous field was well justified.

Small oscillations with the frequency ν in the inhomogeneous AC monopole field.- If an ion travels deeper into the field, the distance $\bar{y}$ from the axis can be quite different from the value $\bar{y}_o$ near the entrance. The inhomogeneousness of the field has to be considered now. The amplitude of the oscillations is now proportional to the field strength which is proportional to $\bar{y}$. Therefore, Equation (15) can be generalized to

$$y = \bar{y} - \bar{y} \; 0.5 \; q \cos(\phi_o + \omega t) \tag{16}$$

where $\bar{y}$ is the distance between an ion and the axis of the instrument, averaged over one AC cycle. This can be anywhere in the inhomogeneous field. $\bar{y}$ (z) describes the centerline about which the small oscillations take place.

The importance of the small oscillation, as described by Equation (16), comes from the fact that they provide the focusing force for the quadrupole or monopole field. Because the field strength is proportional to y, the force is larger during the part of the orbit where y is larger than $\bar{y}$, and vice versa. The average value of the acceleration in the y direction during one cycle of the RF field can be calculated from Equation (10) by use of Equation (16).

$$\ddot{\bar{y}}_{AC} = \frac{1}{\tau}\int_o^\tau \ddot{y}\, dt = \frac{1}{\tau}\int_o^\tau \left[(\bar{y}-\bar{y}\; 0.5 \; q \cos(\phi_o + \omega t)\right] 0.5 \; \omega^2 q \cos(\phi_o+\omega t)\, dt$$

$$\ddot{\bar{y}}_{AC} = -\bar{y}\; 0.125 \; \omega^2 \; q^2 \tag{17}$$

One sees that the average acceleration caused by the AC field is negative and therefore directed toward the axis. It is proportional to the distance $\bar{y}$ from the axis and represents the focusing force of the monopole filter.

Large oscillations with the low frequency $\beta\nu$ in the complete monopole field.- The right side of Equation (6) consists of three terms: The acceleration caused by the DC field, the AC field and the magnetic

field. So far we have only calculated the contribution of the AC field. We have to study now the combined effect of all three fields. The calculation is greatly simplified if we replace the second term, describing the momentary AC acceleration $\ddot{y}_{AC}$, by its average value $\overline{\ddot{y}_{AC}}$ as derived in Equation (17). At the same time we rename the variable y to $\bar{y}$. This results in:

$$\ddot{\bar{y}} = \bar{y}\ 0.25\ \omega^2\ a - \bar{y}\ 0.125\ \omega^2 q^2 + (e/m)^{3/2}\ \sqrt{E/150}\ (H/c)$$

The last term represents the acceleration by the magnetic field alone which we will call

$$B = (e/m)^{3/2}\ \sqrt{E/150}\ (H/c) \tag{18}$$

The first two terms can be combined if we introduce the new parameter

$$\beta^2 = 0.5q^2 - a \tag{19}$$

and the new circular frequency

$$\Omega = 0.5\ \omega\ \beta \tag{20}$$

which results in

$$\ddot{\bar{y}} = -\bar{y}\ \Omega^2 + B \tag{21}$$

We have now to investigate the following three cases:

$$\beta^2 > 0 \qquad \beta^2 = 0 \qquad \text{and} \quad \beta^2 < 0$$

(1) Case $\beta^2 > 0$ Periodic solutions

In this case Equation (21) describes a harmonic oscillator and the solution is given by

$$\bar{y} = \bar{y}_o \cos \Omega t + \dot{\bar{y}}_o\ \Omega^{-1} \sin \Omega t + B\ \Omega^{-2}\ (1 - \cos \Omega t) \tag{22}$$

One can easily verify that Equation (21) is fulfilled and that for $t = 0$ $\bar{y} = \bar{y}_o$ and $\dot{\bar{y}} = \dot{\bar{y}}_o$. These initial conditions inside the field are re-

lated to the corresponding values outside the field by the Equations (13) and (14) which have been previously derived.

One can see that the magnetic field has shifted the center-line of these oscillations from zero to $B\ \Omega^{-2}$.

The frequency of these oscillations is much lower than the frequency of the AC field. It depends upon the operating voltages of the monopole filter which are related to a and q by the Equations (7) and (8). If the DC voltage is increased, its defocussing force reduces the focussing force of the AC field which results in a lower frequency of this oscillation. We will see later that good mass resolution is achieved only if both forces almost compensate each other. In this case β becomes very small.

Let us call R the ratio between the DC voltage U and the AC voltage V:

$$R = U/V \tag{23}$$

During a normal mass scan, this ratio is kept constant. We call U_o the DC voltage for which the focussing and defocussing forces are equal, resulting $\beta = 0$. In this case, ions can pass the filter. From Equations (7), (8), (19) and (23) one obtains

$$U_o = U^* R^2 M \tag{24}$$

One sees that the required voltages are proportional to the mass number M.

If we consider only ions of a single mass number and increase U to $U_o + \Delta U$ and accordingly V by $\Delta V = \Delta U/R$, then β is no longer zero but has the value

$$\beta^2 = 8R^2\ (\Delta U/U_o)(1 + \Delta U/U_o) \tag{25}$$

One sees that β^2 is essentially a measure of the relative deviation from the equilibrium voltage adjustment.

(2) Case $\beta^2 = 0$. Limit of Periodic Solutions

This is the border case between the so-called "stable" and "unstable" solutions. The focussing force of the AC field and the defocussing force of the DC field balance each other. Only the last term in Equation (21) remains and the solution is given by:

$$\bar{y} = \bar{y}_o + \dot{\bar{y}}_o t + 0.5\ B\ t^2 \tag{26}$$

This equation describes a parabolic orbit caused by the magnetic field. (Actually the orbit is circular but the deflection is so small that the deviation from the parabola can be neglected.) Equation (26) can be also derived from Equation (22) by developing the trigonometric functions into series and reducing Ω to zero.

(3) Case $\beta^2 < 0$. Hyperbolic Solutions

In this case we define

$$\mu^2 = a - 0.5q^2 = -\beta^2 \tag{27}$$

and

$$\psi = 0.5\ \omega\ \mu \tag{28}$$

The equation of motion becomes

$$\ddot{\bar{y}} = + \bar{y}\ \psi^2 + B \tag{29}$$

This equation is similar to Equation (21) beside the opposite sign of the $\bar{y}$ term. The solution is no longer periodic and increases exponentially with time. It can be best expressed by:

$$\bar{y} = \bar{y}_o \cosh \psi t + \dot{\bar{y}}_o\ \psi^{-1} \sinh \psi t + B\ \psi^{-2}\ (-1 + \cosh \psi t) \tag{30}$$

These solutions have been ignored so far since for most ions $\bar{y}$ becomes so large that they strike the rod and are removed from the beam. However, it will be shown later that some of these ions can pass the filter and do contribute to the peak tail.

Ion orbits in the monopole field.- An ion that enters the monopole field at the time $t = 0$ with the velocity v (Equation 13) will be at the time $t = z/v$ in position z. It will reach the end of the field $z = L$ after having spent

$$N = \nu\ L \sqrt{150\ m_I/e}\ \sqrt{M/E} \tag{31}$$

cycles in the AC field.

N is mass dependent if E is kept constant. N becomes independent of the mass if E is changed proportional to M. Figure 3 shows N as a function of E for several values of M calculated for the laboratory model monopole filter which had the parameters ν = 1.8 MC and L = 22.2 cm.

It should be emphasized that N is in no way affected by the voltages U and V which are supplied to the rod electrode.

We can now eliminate the time in Equations (16), (22) and (30) by use of

$$\omega t = 2\pi N z/L \tag{32}$$

and obtain the ion orbits:

$$y(z) = \bar{y}(z) \left[1 - 0.5\, q \cos\left(\phi_o + 2\pi N z/L\right)\right] \tag{33}$$

$$\bar{y}(z) = \bar{y}_o \cos \pi\beta N z/L + \dot{\bar{y}}_o (\pi\beta\nu)^{-1} \sin \pi\beta N z/L) + \tag{34}$$

$$+B (\pi\beta\nu)^{-2} \left[1 - \cos \pi\beta N z/L\right]$$

for $\beta^2 > 0$, or

$$\bar{y}(z) = \bar{y}_o \cosh \pi\mu N z/L + \dot{\bar{y}}_o (\pi\mu\nu)^{-1} \sinh \pi\mu N z/L + \tag{35}$$

$$+B (\pi\mu\nu)^{-2} \left[-1 + \cosh \pi\mu N z/L\right]$$

for $\beta^2 = -\mu^2 < 0$.

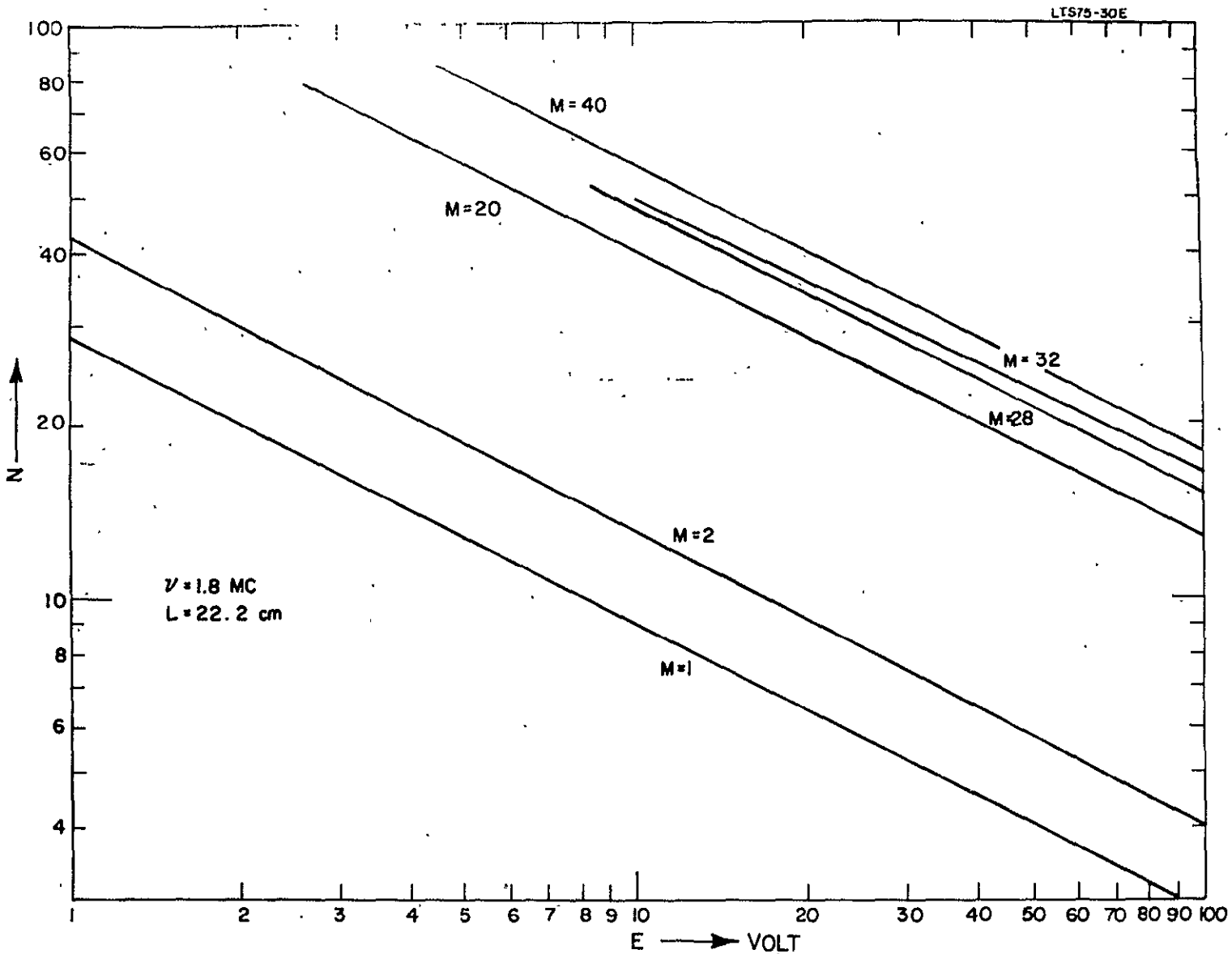

Figure 3. Number N of RF cycles required for an ion of mass number M and acceleration voltage E to pass the monopole filter.

Discussions of the ion orbits.- In order to simplify the understanding of the monopole filter we will proceed in several steps. First, we assume the ordinary case without a magnetic field. Therefore, the last term in Equation (34) and (35) disappears. We assume further that all ions enter the field at the point y_o and parallel to the axis ($\alpha = 0$) which results in the following idealized case.

Infinitesimal entrance aperture.- Combining Equations (33), (13), and (14) with (34) or (35) and setting $\alpha = 0$ results in:

$$y/y_o = C\ [\cos\ (\pi\beta Nz/L) - (q/\beta)\ \sin\ \phi_o\ \sin\ (\pi\beta Nz/L)\ ] \quad \text{for } \beta^2 > 0 \tag{36}$$

$$y/y_o = C\ [1 - (q\pi Nz/L)\ \sin\ \phi_o\ ] \qquad \text{for } \beta = 0 \tag{37}$$

and

$$y/y_o = C\ [\cosh\ (\pi\mu Nz/L) - (q/\mu)\ \sin\ \phi_o\ \sinh\ (\pi\mu Nz/L)] \text{ for } \mu^2 > 0 \tag{38}$$

where

$$C = [1 - 0.5 q\ \cos\ (\phi_o + 2\pi Nz/L)\ ]/\ [1 - 0.5\ q\ \cos\ \phi_o\ ] \tag{39}$$

is a function of ϕ_o and z. However, since q is small C does not deviate much from one. For the first approximation we neglect this deviation and assume C = 1. The effect of C will be discussed later.

One can easily verify that for z = 0 ... $y = y_o$. Let us first discuss the periodic solutions of Equation (36). Since ions enter the field at any time, y is in general a function of ϕ_o and oscillates with the AC frequency ν. Only those ions can pass the filter for which $y > 0$ for any value of z. The amplitude of the oscillation is a maximum if $\beta Nz/L = 1/2$. In this case the first term becomes zero and ϕ_o must be between π and 2π. The amplitude of the oscillations becomes zero if $\beta Nz/L = 1$. However, in this case the cos-term becomes -1 and $y = -y_o$; therefore all these ions strike the V-electrode and are absorbed. At the exit aperture, (z = L), $\beta Nz/L$ must be slightly smaller than 1 to permit ions to pass. y has a

maximum for $\phi_o = 3\pi/2$. Therefore, the maximum value of β for which $y \geq 0$ is obtained from Equation (36) for $\phi_o = 3\pi/z$ which results in:

$$q\ \pi\ N = -\pi\ \beta_{max}\ N \cot\ (\pi\ \beta_{max}\ N) \tag{40}$$

or, since $\beta_{max}N$ is almost one, in:

$$\beta_{max} = q\pi/(1 + q\pi N) \tag{41}$$

The first condition that an ion can pass the filter is that it does not strike the V-electrode. Not all ions for which $\beta < \beta_{max}$ can pass the filter without striking the V-electrode. They must enter the field when the phase angle is between the limits

$$(3\pi/2 - \Delta\phi_1) < \phi_o < (3\pi/2 + \Delta\phi_1) \tag{42}$$

where $\Delta\phi_1$ is derived from Equations (36) and (37) for $y = 0$ and $z = L$. One obtains for $\beta^2 > 0$

$$\cos\ \Delta\phi_1 = -(\beta/q)\ \cos\ (\pi\beta N)\ /\sin\ (\pi\beta N) \tag{43}$$

and for $\beta^2 = -\mu^2 < 0$

$$\cos\ \Delta\phi_1 = -(\mu/q)\ \cosh\ (\pi\mu N)\ /\sinh\ (\pi\mu N) \tag{44}$$

It shall be mentioned that $\Delta\phi_1$ does not depend on y_o and only slightly on q. $\Delta\phi_1$ is zero for $\beta = \beta_{max}$ and increases steadily with decreasing β and increasing μ. For $\beta N = 1/2$ one obtains $\Delta\phi_1 = \pi/2$. For $\beta = 0$ and large values of N $\Delta\phi_1$ becomes slightly larger than $\pi/2$. Finally $\Delta\phi_1$ becomes π for μ slightly smaller than q and stays constant for larger values of μ. In this case the attraction toward the rod, due to the large DC voltage, is so great that the beam no longer strikes the V-electrode.

Equation (41) is only the condition under which an ion does not strike the V-electrode. This is not enough if an ion should pass the filter.

A second condition has to be fulfilled which requires that the ion does not strike the exit aperture. This means that at the end of the field (z = L) the distance y from the axis must be smaller than the height h_2 of the exit aperture. Again the largest value of y occurs at the phase angle $\phi_o = 3\pi/2$. If for this angle $y_{max} < h_2$ no ions will strike the exit aperture. However, if $y_{max} > h_2$ only ions within the phase angles

$$\phi_o < (3\pi/2 - \Delta\phi_2) \text{ and } \phi_o > (3\pi/2 + \Delta\phi_2) \qquad (45)$$

can pass the exit aperture. $\Delta\phi_2$ can be calculated from Equations (36) and (37) by replacing $y = h_2$ and $z = L$ which results in:

$$\cos \Delta\phi_2 = (\beta/q) \left[h_2 / (y_o C) - \cos(\pi\beta N)\right] / \sin(\pi\beta N) \text{ for } \beta^2 > 0 \qquad (46)$$

$$\cos \Delta\phi_2 = (\mu/q) \left[h_2 / (y_o C) - \cosh(\pi\mu N)\right] / \sinh(\pi\mu N) \text{ for } \beta^2 = -\mu^2 < 0 \qquad (47)$$

Equations (45), (46) and (47) are the conditions for an ion to pass the exit aperture. In addition to this, it is possible that ions are removed by the rod. Especially ions which are nearly focused at the end of the V-electrode (βN almost 1) have a very large amplitude near the center of the field. They can pass the rod electrode if $y < r_o$, or within the phase angles

$$\phi_o < (3\pi/z - \Delta\phi_3) \text{ and } \phi_o > (3\pi/z + \Delta\phi_3) \qquad (48)$$

The angle $\Delta\phi_3$ can be calculated from Equation (37). y becomes a maximum if $\beta N z/L = 1/2$; in this case the cosine becomes zero and the sine one. This occurs within the field if $z < L$ or for $\beta N > 0.5$. One obtains:

$$y/y_o = -C\,(q/\beta)\,\sin\phi_o \tag{49}$$

or

$$\cos\Delta\phi_3 = (\beta/q)\,r_o/(y_o C) \tag{50}$$

If the right sides of this equation become one, then $\Delta\phi_3$ becomes zero and all ions can pass. This is also true if r_o is further increased or y_o reduced and the right side of Equation (50) becomes larger than one. However, if β becomes smaller then the right side of Equation (50) becomes smaller than one and some ions are liminated by the rod. Therefore, only ions can pass the hole filter which enter the field when the phase angle is within the limits

$$(3\pi/2 - \Delta\phi_1) < \phi < (3\phi/2 - \frac{\Delta\phi_2}{\Delta\phi_3}) \text{ and } (3\pi/2 + \frac{\Delta\phi_2}{\Delta\phi_3}) < \phi_o < (3\pi/2 + \Delta\phi_1) \tag{51}$$

in which Equations the larger one of the two angles $\Delta\phi_2$ and $\Delta\phi_3$ has to be used.

The transmission $T(y_o)$ of the filter for ions entering at y_o is defined as the ratio of the phase angles for which ions can pass to the total phase angle introduced (2π). One obtains:

$$T(y_o) = (\Delta\phi_1 - \frac{\Delta\phi_2}{\Delta\phi_3})/\pi \quad \text{(use the larger value of } \Delta\phi_2 \text{ or } \Delta\phi_3) \tag{52}$$

If $\Delta\phi_2$ becomes equal to π no ion can pass the filter; they are so much attracted by the rod that all strike the exit aperture. Since N is large one obtains from Equation (47)

$$\mu_{max} \approx q \tag{53}$$

which determines the length of the peak tail towards lighter masses.

Figure 4 shows $\Delta\phi_1$, $\Delta\phi_2$, and $\Delta\phi_3$ calculated for the laboratory instrument for N = 10 and $h_2/y_o C$ = 1, 2, 5, 10, 20. For the abscissa of this

figure $(\beta N)^2$ has been chosen which is proportional to the detuning of the instrument. By the use of Equations (25), (31), (24) and (4) it is possible to express this important parameter $(\beta N)^2$ in the simple form:

$$(\beta N)^2 = (\pi\alpha_o)^{-2} \, (\Delta U/E)(1 + \Delta U/U_o) \qquad (54)$$

The form factor of the field ($\alpha_o = r_o/L$) is a constant. As long as $\Delta U \ll U_o$, the last term may be neglected and $(\beta N)^2$ is only proportional to ΔU and inverse proportional to E. It is independent of all other operating parameters M, U_o, V_o, R and ν.

The transmission $T(y_o)$ is plotted in Figure 5 for N = 10 and for the values y_o/r_o = 0.05, 0.1, 0.2, 0.5, 1. These curves represent the shape of individual mass peaks. The full drawn lines represent the peak shape if no special exit aperture is used $y_2 = r_o$. The interrupted lines indicate the effect of an exit aperture smaller than r_o. Figure 6 shows the transmission for $y_o/r_o = 0.1$, $h_2 = r_o$ and the values N = 5, 10 and 20. The following conclusions can be drawn.

(1) The peak shapes are assymetric with a sharp edge on the high mass side and a long tail at the low mass side. This tail extends far beyond the "stability limit" $\beta = 0$ and can be reduced if $h_2 \ll r_o$.

(2) The maximum transmission stays fairly constant for $y_o/r_o < 0.1$ and decreases rapidly for higher values of y_o.

(3) The peak width at half height for $y_o/r_o = 0.1$ is $\Delta(\beta N)^2 = 0.72$ if no exit aperture is used. It increases only slightly for smaller values of y_o or N. A smaller exit aperture reduces the peak width and the peak tail significantly without much loss of transmission as long as $h_2/r_o > 0.2$. The peak width is proportional to the ion energy E and to the square of the acceptance angle α_o. In order to obtain high resolution it is therefore necessary to use a long and narrow monopole field ($L \gg r_o$) and to work with slow ions. The peak width ΔU does not depend on the mass nor on the operating conditions of the monopole filter. Therefore, the resolution $M/\Delta M$ is not constant as in magnetic mass spectrometers but is rather proportional to M. This is a definite advantage since the resolution is highest for high masses where it is needed most.

(4) The location of maximum intensity of a mass peak does not occur at $\beta = 0$, corresponding to a linear mass scale, but is shifted toward higher masses. If one considers the center of the half height as the location of the asymmetrical peak and assumes $h_2 = r_o$ and $y_o/r_o = 0.1$ then this shift is

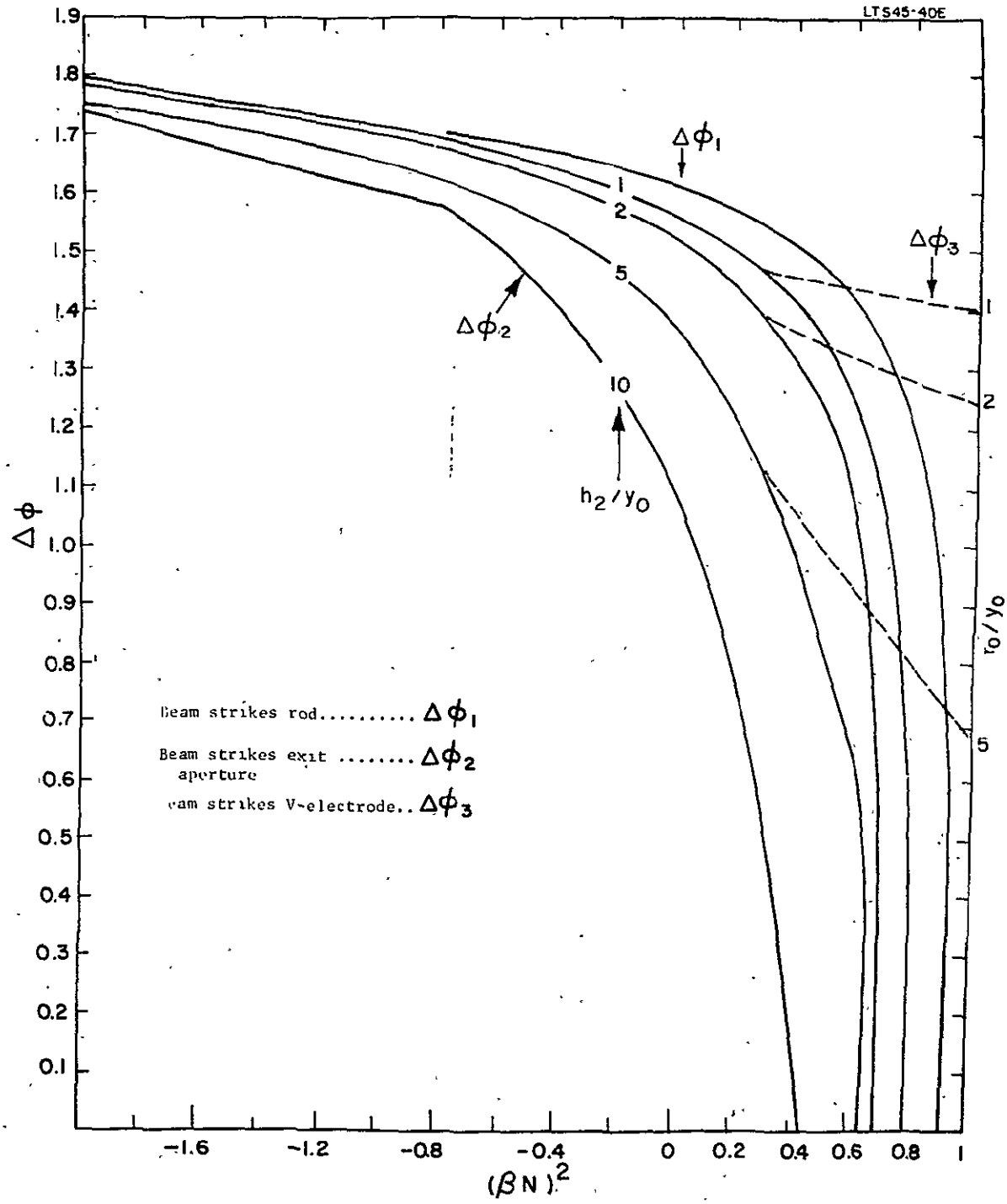

Figure 4. $\Delta\phi_1$, $\Delta\phi_2$, $\Delta\phi_3$ as functions of $(\beta N)^2$.

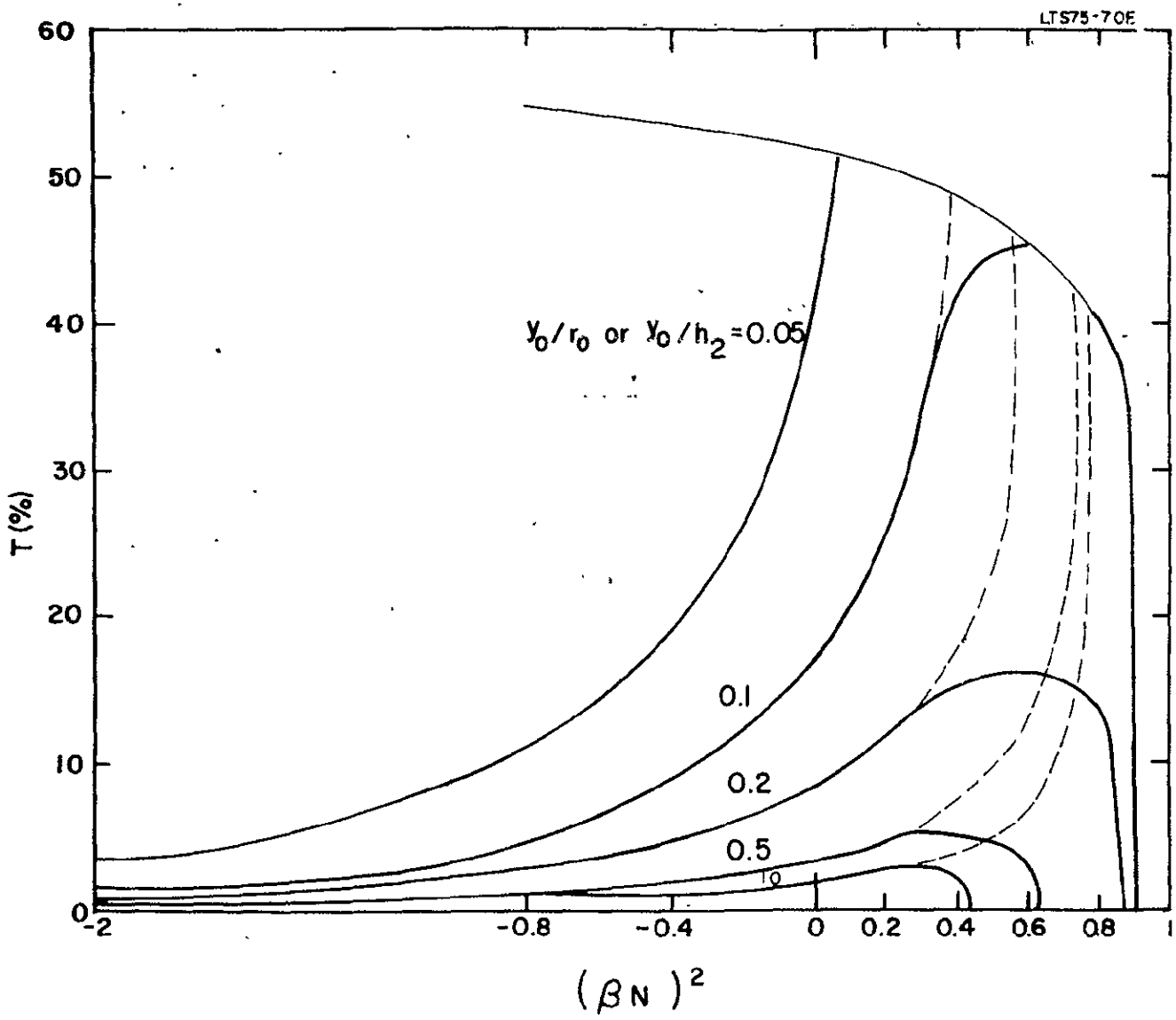

Figure 5. Transmission for N = 10, y_o/r_o = 0.05, 0.1, 0.2, 0.5, 1.

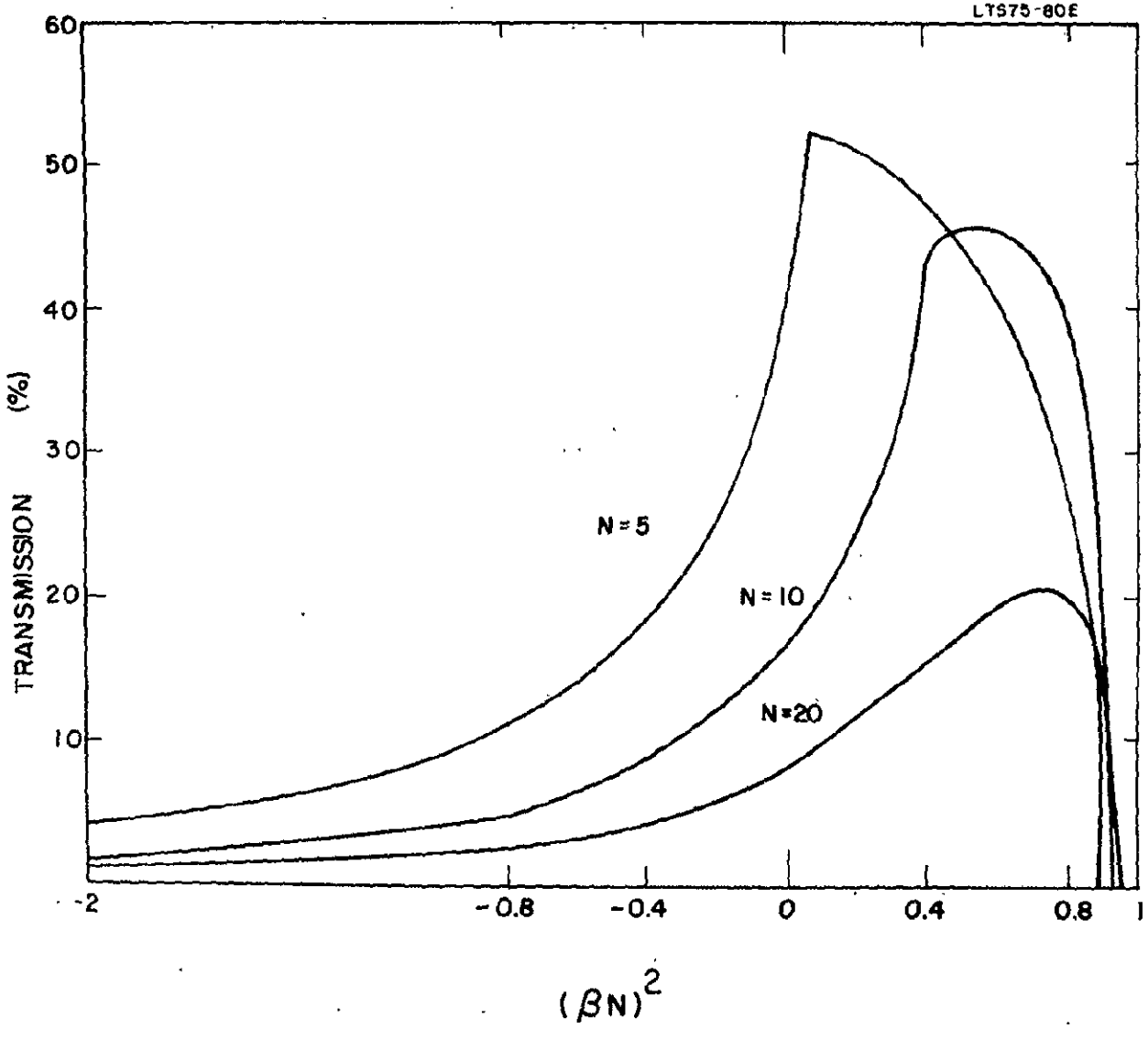

Figure 6. Transmission for $v_\parallel/r = 0.1$, $h = r$, $N = 5, 10, 20$.

$(\beta_p N)^2 = 0.3$, 0.5 for N = 5 and 10 and stays practically constant for larger N. A smaller exit aperture suppresses the left side of the peak and shifts the center of gravity toward higher masses. For instance, if N = 10, $y_o/r_o = 0.1$ and $y_o/h_2 = 0.5$ or $h_2/r_o = 0.2$ one obtains $(\beta_p N)^2 = 0.8$. This shift is proportional to the acceleration voltage E of the ions and is independent of the mass number and the operating parameters of the monopole filter. However, it is proportional to the square of the maximum acceptance angle α_o.

Finite entrance aperture.- In order to obtain adequate sensitivity it is necessary to increase the size of the entrance aperture as much as possible. The shape of the entrance aperture can be circular with the center in the axis or offset such that no part of the aperture is obstructed by the V-electrode. A triangular shape of the entrance aperture has been chosen for the laboratory model because this permits easy variation of the size by moving the hypotenuse of the triangle. Since in this case the width of the beam is proportional to y_o one obtains the total transmission

$$T = 2\, h_1^{-2} \int_0^{h_1} h_o\, T\,(h_o)\, d\, h_o \qquad (55)$$

The accurate calculation of this integral is difficult and hardly worth the trouble since it does not reveal any new features. The product $h_o\ T\ (h_o)$ is small for small values of h_o, has a broad maximum for $h_o/r_o = 0.1$ to 0.2 and becomes small again for larger values of h_o/r_o. Therefore an entrance aperture larger than $h_1/r_o = 0.2$ has little effect on the sensitivity but increases the background caused by reflected stray ions. Therefore for practical purposes $h_1/r_o = 0.2$ is the useful limit of the entrance aperture. In this case the total transmission becomes practically the same as the transmission T $(y_o/r_o = 0.1)$ for the center of the entrance aperture which has been calculated previously. The discussions about mass scale and resolution will be based on this curve.

So far we have assumed that a parallel beam with $\alpha = 0$ enters the field. This assumption was well justified since the angular beam spread is small compared with the deflection near the field entrance. We see from Equations (14) and (34) that the α term contributes $\alpha v(\pi\beta\gamma)^{-1} \sin \pi\beta Nz/L$ to the total deflection. This becomes zero and independent of α if $\beta Nz/L = 1$. We have seen previously that for z = L and $\beta N = 1$ ... $y = -y_o$ independent of the phase of the field at the moment of entry. Now we see that for the same condition the α term vanishes. Therefore a reversed real image of the entrance aperture is produced at this spot. This image actually exists in a quadrupole instrument where ions can freely cross the axis. In a monopole instrument βN must be slightly smaller than one to prevent ion impact on the V-electrode and the image is formed outside after the filter. Since the exit aperture is not too far before this image,

the beam is well compressed there, which results in much higher signals if the monopole filter is in operation compared to grounded electrodes, corresponding to the zero point of the mass scale. This is in good agreement with experimental observations.

Sensitivity variations due to the small oscillations.- So far we have neglected the small oscillations and have assumed that C = 1. A more accurate calculation requires closer attention to the factor C. For the end of the field z = L we obtain from Equation (39)..

$$C = [1 - 0.5\ q \cos(\phi_o + 2\pi N)] / [1 - 0.5\ q \cos \phi_o] \qquad (56)$$

Let us consider the following four characteristic cases:

Case 1: For N = 1, 2, 3 ... C_1 is independent of ϕ_o and $C_1 = 1$.

Case 2: For N = 1/2, 3/2, 5/2 ... $C_2 = \dfrac{1 + 0.5\ q \cos \phi_o}{1 - 0.5\ q \cos \phi_o} \approx 1 + q \cos \phi_1$

Case 3: For N = 1/4, 5/4, 9/4 ... $C_3 = [1 + 0.5\ q \sin \phi_o] / (1 - 0.5\ q \cos \phi_o$

$$\approx 1 + 0.5\ q\ (\sin \phi_o + \cos \phi_o)$$

$$C_3 = 1 + 0.5\ q \sqrt{2} \cos(\phi_o - \pi/4)$$

Case 4: For N = 3/4, 7/4, 11/4 ... $C_4 = [1 - 0.5\ q \sin \phi_o] / (1 - 0.5\ q \cos \phi_o$

$$\approx 1 + 0.5\ q\ (-\sin \phi_o + \cos \phi_o)$$

$$C_4 = 1 + 0.5\ q \sqrt{2} \cos(\phi_o + \pi/4)$$

Figure 7 shows $C(\phi_o)$ for these typical cases. The important region of these curves is around $\phi_o = 3\pi/2$. For this angle one obtains:

$$C_3 = 1 - 0.5\ q \qquad \text{and} \qquad C_4 = 1 + 0.5\ q$$

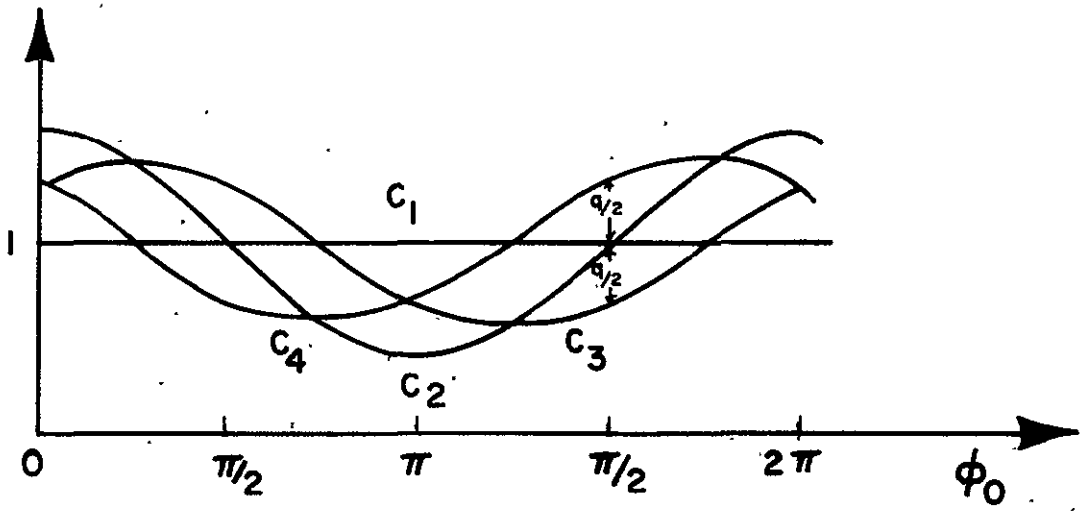

Figure 7. Small oscillations C in dependence of entrance phase ϕ_o for q = 0.6.

Assuming the same value of q = 0.64 which has been used previously, this results in $C_3 = 0.68$ and $C_4 = 1.32$. The accurate calculation of the phase angles where ions are transmitted is now much more complicated since C is also a function of ϕ_o. However, one can obtain a good approximation if one assumes C to be constant with the values C_3 and C_4 mentioned above. Figure 8 shows the peak shape for these two cases, calculated in the same manner as previously. One sees that the transmission for Case 3 is about 10 percent larger than for Case 4. This means that the sensitivity of the monopole mass spectrometer is a periodic function of N. If as usual, the acceleration voltage is kept constant the sensitivity becomes mass dependent. If, for instance, the ratio O_2/N_2 in air is measured it can happen that at one accelerating voltage the sensitivity for O_2 is a maximum and for N_2 near a minimum and vice versa for another voltage. This results in peak height ratios which depend strongly on the accelerating voltage. We will see later that this undesirable effect has been really observed and is even larger than calculated here because of a similar effect caused by oscillations in the x-direction. The instrument is still useful for quantitative work if the sensitivity is calibrated for each individual mass number at exactly the same accelerating voltage as used during the analysis.

The sensitivity becomes independent of the mass if the accelerating voltage is increased proportional to the mass since in this case N becomes a constant. Unfortunately this results in constant resolution $M/\Delta M$, which means that the peak width increases proportionally to the mass. Under these conditions it is difficult to achieve unit mass resolution for high masses. In addition the peaks at low mass numbers are unnecessarily too sharp which limits the maximum scanning speed permissible if peak clipping has to be avoided.

Since the sensitivity variations are caused by the exit aperture, they can be reduced to practically zero if the exit aperture is opened to the full width of the rod distance r_o. Unfortunately in this case the peak tail becomes rather large. Therefore a compromise is necessary. Entrance and exit apertures should be chosen as large as compatible with adequate resolution and sufficiently low background. By this choice, and by operating the instrument with a low voltage ratios R, it is possible to keep the sensitivity variations within tolerable limits.

Effect of the magnetic field.- Let us call D_o the deflection of the beam at the end of the filter caused by the magnetic field alone. From Equation (26) we obtain

$$D_o = 0.5\ B\ t^2$$

If we use $t = L/v$ and Equations (3) and (18) we obtain

$$D_o = (0.5c)\sqrt{150\ e/m_1}\ \ L^2H/\sqrt{ME} \qquad (57)$$

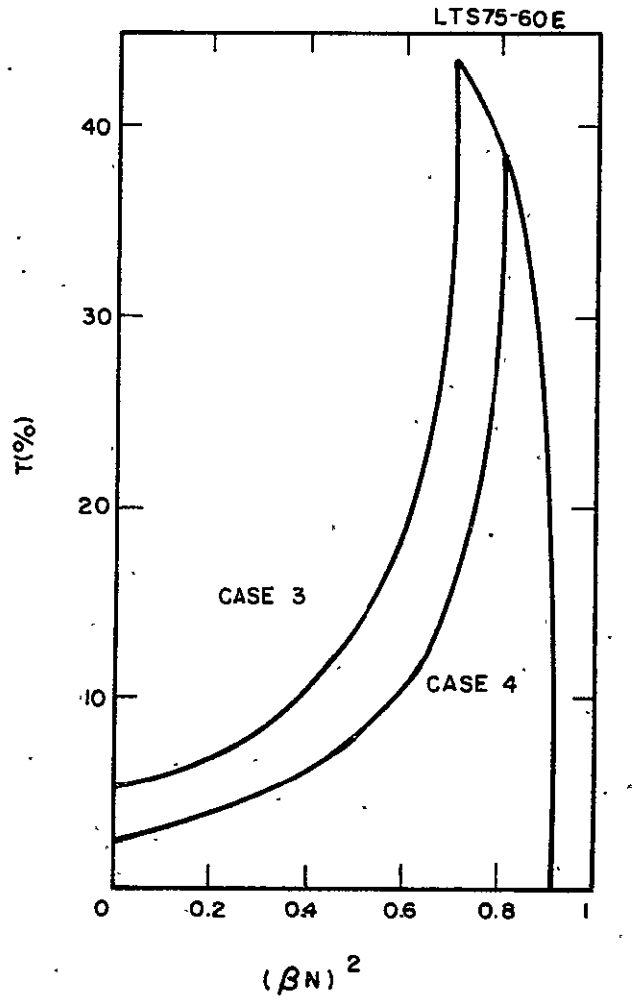

Figure 8. Peak shapes.

The factor has the value

$$0.5c\sqrt{150\ e/m} = 3.45 \times 10^{-3}$$

For example one obtains for M = 28, E = 25 volts, H = 5 gauss and L = 22.2 cm, the total deflection D_o = 0.3 cm. This deflection is obtained either when the rod is connected to the V-electrode, or for $\beta = 0$ in which case the AC focussing force is equal to the DC defocusing force. If the focussing force is larger than the defocussing force then β is positive and we have to use Equation (34) to obtain the magnetic deflection. From the last term we obtain for z = L

$$D = B(\pi\beta\nu)^{-2}\ (1 - \cos\ \pi\beta N)$$

which can be expressed by Equation (57) in the form

$$D = D_o\ 2(\pi\beta N)^{-2}\ (1 - \cos\ \pi\beta N) \qquad (58)$$

For the focus point $\beta N = 1$ one obtains $D = D_o\ 4/\pi^2$. One can see that the focussing force of the monopole field reduces the magnetic deflection to about one half of its original value.

We have seen previously that for $\beta N = 1$ a well focused image of the entrance aperture would occur if the beam would not strike the V-electrode. The effect of the magnetic field is to shift this image from negative to positive y-values where it really can be used. Accurate calculation of the transmission under this condition becomes very complicated. Because the deflection of the beam is gradual, one must expect that still almost one half of the beam is lost at the V-electrode near the entrance aperture. Therefore, the sensitivity gain should be quite moderate. However, a very substantial gain has been observed as can be seen from Figure 9 which shows two spectra, one without and one with a magnet, but otherwise obtained under identical conditions.

It has been found experimentally that the imposition of such a magnetic field increases the peak heights by a factor of 10 more or less.

This result might be questioned since the imposed field could have increased the output of the Nier type ion source. The direction of the field is parallel to the electron beam and prevents its spread, thus improving the ion source output. A field in the opposite direction should have the same effect on the ion source, but actually, the peak heights were observed to decrease by about an order of magnitude. This indicates clearly that the observed effect is attributable primarily to the ion beam deflection.

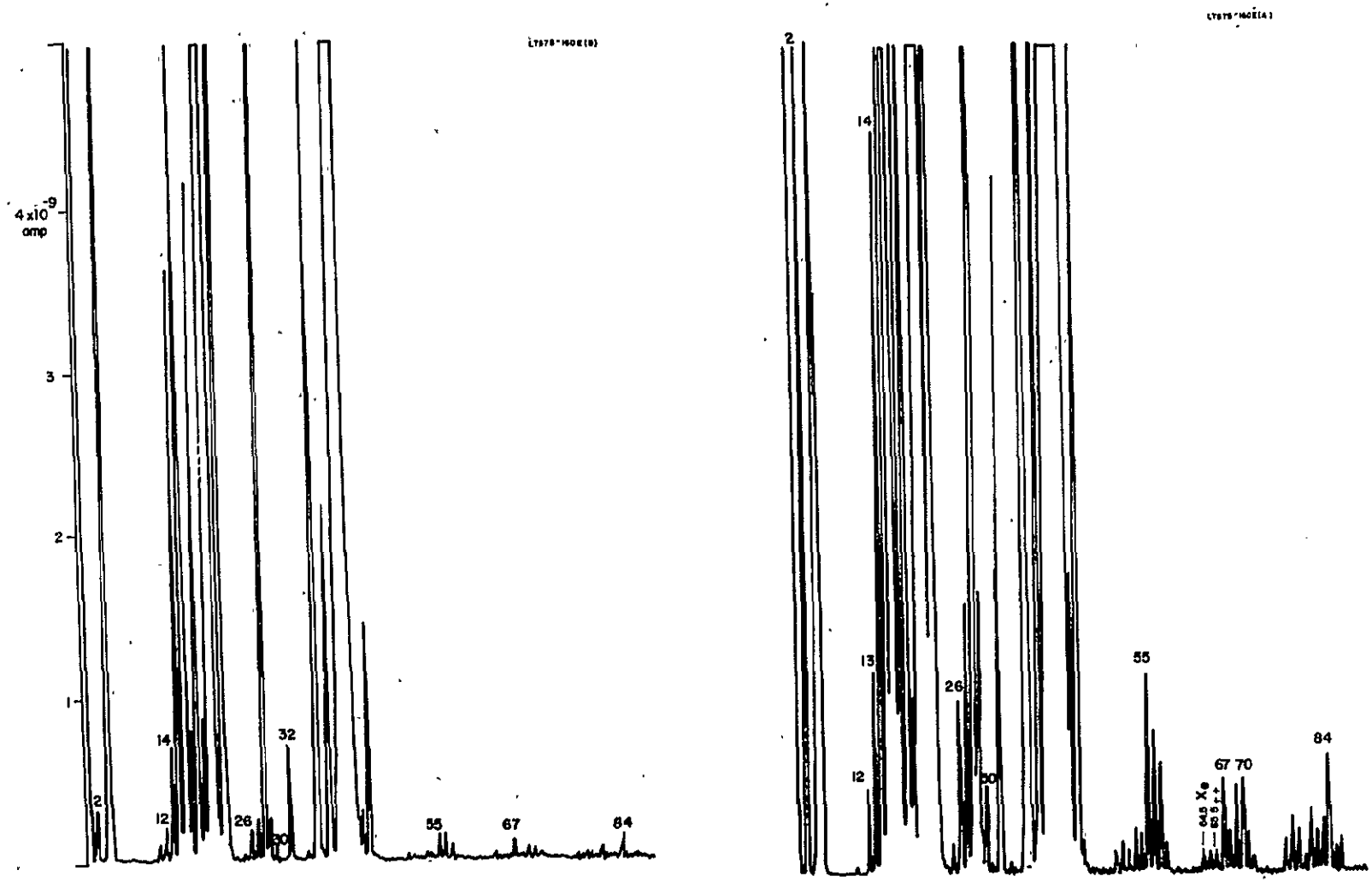

Figures 9a and 9b. Two spectra with and without magnet field.

For these experiments the magnetic field was produced by a 5-inch bar magnet located near the entrance aperture of the monopole instrument at a distance of approximately 4-1/2 inches from the axis. The field strength at the entrance aperture was approximately 7.5 gauss and diminished gradually towards the exit aperture. The ion accelerating voltage was 25 volts, which results in a deflection D_o = 0.3 cm at the end of the field for ions of a medium mass 28. This indicates that a relatively slight beam deflection is sufficient to produce the desired effect. This deflection has to be gradual and distributed over a large part of the beam and cannot be replaced by an electrical beam deflection before the entrance aperture. The optimum magnet location which produces the largest peak heights is very slightly mass dependent. It has been found experimentally that it is better to have the largest field near the entrance aperture than a homogeneous field along the whole monopole. Fortunately, positioning of the magnet is not critical since significant sensitivity improvements can be realized over the mass range from mass 2 up with one fixed magnet position. However, the degree of sensitivity improvement is slightly mass dependent. Only mass 1 requires a different position of the magnet and the sensitivity gain is small. It should be mentioned too that the magnetic field has no effect on the mass scale nor the peak shape.

The large improvement of the sensitivity can be understood if one considers the focussing effect in the x-direction. Since the magnetic field shifts the image away from the V-electrode, one has to expect that the acceptance angle in the x-direction can be greatly increased before ions strike the two planes of the V-electrode.

D. Accurate Solutions of the Equation of Motion

It is not intended in this report to repeat the development of the accurate solutions which can be found in the literature listed in the references. The effect of the simplifications shall be discussed only qualitatively. We have assumed in a previous section that the field strength is constant over the limited range of the small oscillations. Actually, the field strength increases proportionally to y which produces a nonlinear distortion of the harmonic oscillations. The resulting total oscillation is composed of the one with the base frequency, which was expressed by Equation (10), and others with higher frequencies. In general these frequencies are not exactly harmonics but the deviations from harmonics are quite small. Fortunately, the amplitude of these quasi-harmonic oscillations decrease quite rapidly. For instance, the amplitude of the second harmonic is only 4 percent of the base oscillation. Therefore, the simplifications of the previous section were well justified.

For the accurage solutions one obtains instead of Equation (19) a long series* which has been calculated accurately with a computer and the

*McLachlan[7], Equation (4) 4.79, page 83.

results are shown in Figure 10, the so-called "stability diagram". "Unstable" solutions have been included in this diagram. Comparison with Equation (13) shows that the maximum deviations are only about 4 percent near the top of the diagram. For smaller values of a and q the deviations are even less.

The oscillations in the x-direction are essentially the same as in quadrupole instruments and have therefore not been discussed explicitly in this report. They are also of less importance for the monopole instrument which is normally operated with a much smaller voltage ratio, corresponding to an operating point which is far away from the x-stability limit. In this case, the amplitude of the oscillations in the x-direction is quite small. However, these oscillations are also more restricted by the V-electrode which limits its amplitude to $X_{max} \leq y$. If a beam of finite width is intercepted by the V-electrode near the exit aperture, it must be expected that the cut-off will not be as sharp as shown in Figure 8. This is in close agreement with experiments, where a fairly symmetrical peak shape has been observed if the instrument is operated with adequate resolution.

E. Experimental Performance Tests of the Monopole Mass Spectrometer

Shortly after von Zahn's (Ref. 1) publication about the monopole mass spectrometer appeared, company sponsored research was started to investigate experimentally the performance of a monopole and quadrupole mass spectrometer with the same dimensions. The results of these investigations were reported by R. Herzog (Ref. 8) at the first conference about "Direct Aeronomic Measurements in the Lower Atmosphere" at the University of Illinois in October 1963. The advantages of the monopole instrument were so obvious that the construction of such a flight instrument was proposed to NASA. Unfortunately two years elapsed before this program was funded.

In the meantime, General Electric has put a vacuum analyzer on the market which is based on the monopole principle. In order to permit a quick start of the work, it was decided to purchase one of these vacuum analyzers and use it for the initial tests. Considering that this monopole instrument was one of the first production units, it performed reasonably well. The instrument was originally used on an oil pumped system for the analysis of atomic oxygen beams. The performance deteriorated rapidly, partly due to the contamination of the ion source and of the monopole electrodes with trace amounts of pump oil and partly due to the effect of atomic oxygen on the electrodes of the ion source. The peak size was reduced, the peaks were widened and became irregular in shape and the peak height became very unstable. Cleaning of the instrument and gold plating of the ion source have restored the original performance. However, even with the gold plated electrodes, a slow deterioration of the mass spectra occurred. Finally, the monopole mass spectrometer was installed in an

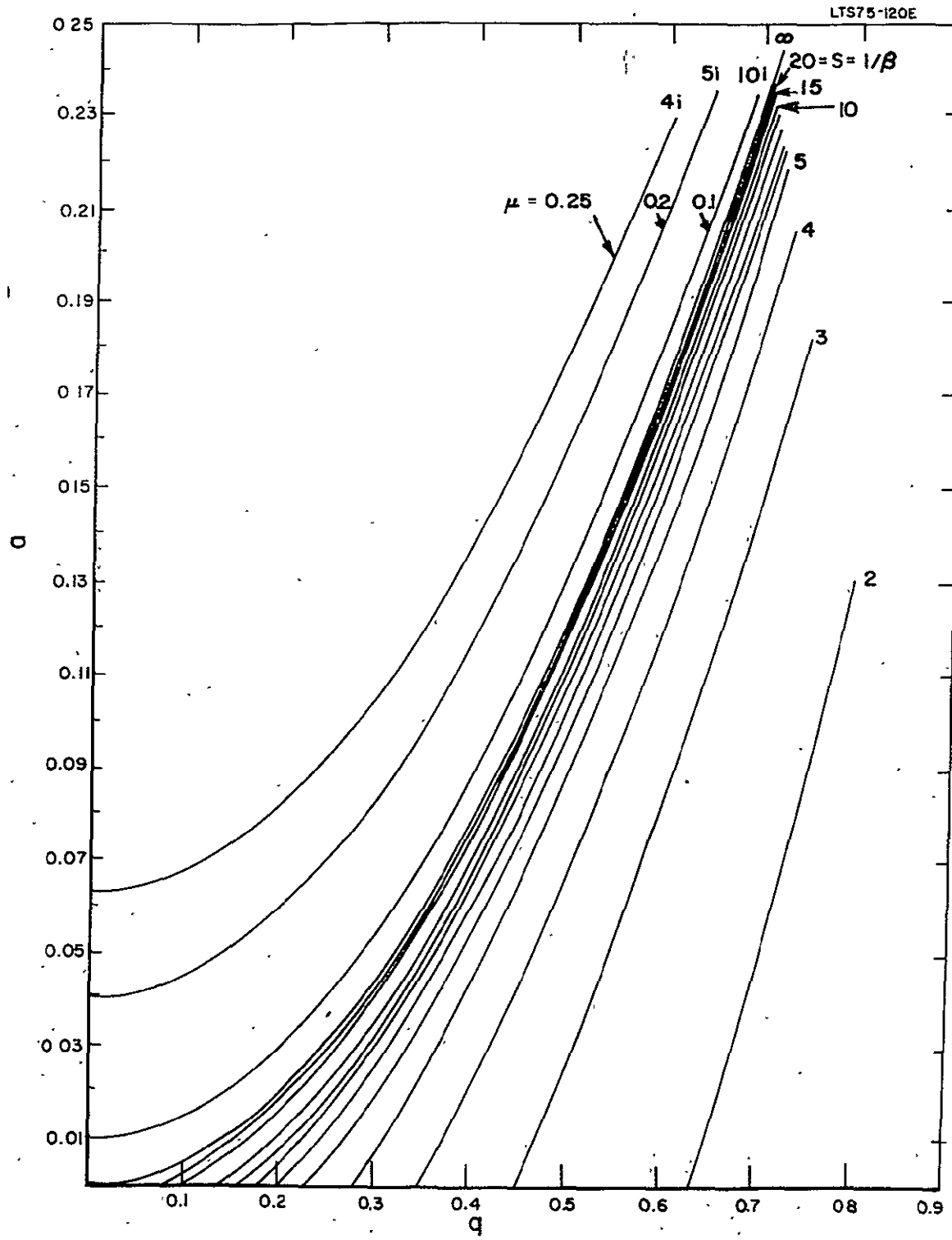

Figure 10. Stability diagram.

oil free, ion pumped, ultra high vacuum system which could be baked at about 400°C. The instrument now worked perfectly stable over a period of many months. During this time, this instrument was mainly utilized to study the performance of the titanium sublimation pump which will be described later.

The General Electric monopole mass spectrometer is equipped with fixed entrance and exit apertures and is operated with two fixed voltage ratios. It can analyze only positive ions. These restrictions did inhibit a thorough investigation of the performance of the monopole mass spectrometer. Therefore, a laboratory model of a monopole mass spectrometer has been designed and built with the following basic parameters:

rod length: $L = 22.2$ cm, field radius: $r_o = 0.762$ cm,
rf frequency: $\nu = 1.8 \times 10^6$ cps

The following design features have been incorporated. Both the entrance and exit aperture are triangular in shape and the height of the triangle is adjustable from outside during the operation of the instrument. The V-electrode is insulated from ground which permits that ions created at ground potential can be accelerated into the monopole analyzer. The entrance aperture is also insulated from ground, which permits deceleration of the ions right after the entrance aperture. A higher gain electron multiplier has been incorporated to permit counting of single ions. For this purpose, a copper beryllium multiplier with 16 dynodes, made by ITT, Model No. F4036, is used. The dark current is negligible and the gain exceeded the specifications and stayed practically constant for about three years. The entrance aperture is the only connection between the ion source region and the analyzer region, which permits differential pumping and the use of a higher pressure in the ion source than in the analyzer. The instrument is still in operation and used to check specific performance capabilities of the monopole mass spectrometer.

The construction of the monopole mass spectrometer has been made according to ultra high vacuum standards. The housing is made of stainless steel with heliarc welded flanges. Only copper gaskets are used. High density aluminum and mica are used for the insulators. The rod- and the V-electrode are gold plated and the entrance and exit aperture and the electrodes of the ion source are made from a thin sheet of solid gold. A rhenium filament has been used to produce the ionizing electron current. The alignment of the rod towards the V-electrode has been done with great care. Deviations from the right position are less than 1 mil. It should be mentioned here that the alignment of a monopole mass spectrometer is by far less critical than the alignment of a quadrupole instrument. If in the later one the field radius changes slightly along the length of the quadrupole, then different sections of the quadrupole are tuned for different masses with the result that none of them can pass the whole filter. If the misalignment is not so strong, then some

ions can pass the filter, but the total intensity will be greatly reduced. In a monopole mass spectrometer, ions stay in the field for only one-half of a major oscillation. Therefore, misalignment can never lead to the elimination of the whole beam. It will result in a slight change of the shape of the major oscillation and have little effect on the actual performance of the instrument.

F. RF Power Supply

The power supply for the laboratory instrument has been built in such a way that it permits testing of the instrument under a wide variety of situations. Any value of the voltage ratio can be adjusted. Normal scan is performed by keeping this voltage ratio constant. The scanning speed can be adjusted over a very wide range. The upper and lower limit of the scan can be adjusted separately. It is possible to use either single scan or automatically repeated scans. In addition, manual adjustment of any peak is possible, and this peak adjustment stays perfectly constant. For the extended mass range to be described later, the AC voltage is kept constant and the DC voltage is reduced. The scanning speed of the extended mass range can be adjusted independently from the scanning of the regular mass range. The extended mass range scan can be started either manually or automatically. Finally, it is possible to reverse the polarity of the DC voltage to permit analysis of negative ions. This power supply will be described below in greater detail. It performed extremely well and reliably for many years and was very convenient for all tests and the routine operation of the monopole mass spectrometer.

General description.- The RF Power Supply is used to generate a regulated 1.8 MC RF signal, amplitude modulated from 2 V p-p to 1800 V p-p, and a superimposed DC signal proportional to this RF amplitude. The power supply consists of two basic parts: the sweep chassis and the RF unit. Many special features are incorporated into this unit which allows the operator complete flexibility in its use.

Circuit description.

Sweep Unit

Refer to simplified schematic, Figure 11.

A basic saw tooth sweep voltage is generated by AR1, a high gain operational amplifier in an integrator circuit. The output is linear with time and the slope is dependent on RC and the applied voltage. The capacitor values are selectable by the front panel coarse speed control which provides the basic ranges of 1, 10, and 100 seconds. The fine speed control permits the selection of intermediate values by changing the input current to the integrator.

The slowest possible speed is approximately 500 seconds. The highest speed is approximately 1 second.

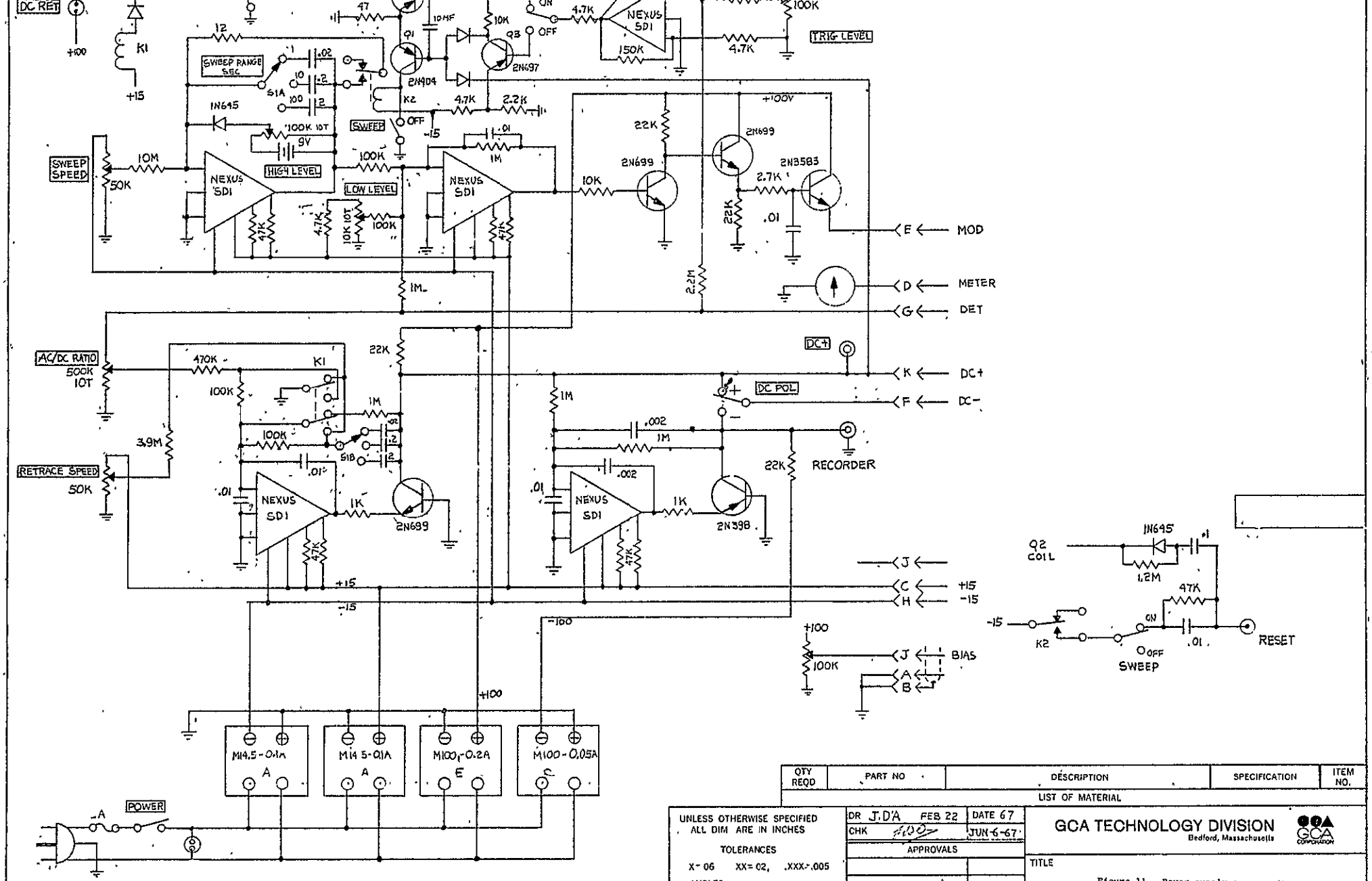

QTY REQD	PART NO	DESCRIPTION	SPECIFICATION	ITEM NO.

LIST OF MATERIAL

UNLESS OTHERWISE SPECIFIED ALL DIM ARE IN INCHES

TOLERANCES

X- 06 XX= 02, .XXX-.005

ANGLES

MACHINE FINISH ✓

BREAK SHARP EDGES AND COR .005 TO .020R APPROX

	DR J.D'A FEB 22	DATE 67
	CHK JUN-6-67	

APPROVALS

RELEASED

MATERIAL

FINAL FINISH

NEXT ASSY | USED ON

APPLICATION

GCA TECHNOLOGY DIVISION
Bedford, Massachusetts

TITLE

Figure 11. Power supply sweep unit.

SIZE	DRAWING NO
C	1-236-200-

SCALE	WT	SHEET OF	REV

DO NOT SCALE

The maximum sweep voltage can be limited to any value within the sweep range by adjusting the "HIGH LEVEL" potentiometer. The generated sweep voltage is applied to the summing junction of a DC amplifier which drives the RF amplifier. The RF amplifier produces a 1.8 MC saw tooth modulated signal which varies between 2 V p-p and 1800 V p-p. A diode rectifier produces a DC voltage proportional to the AC signal with a maximum apmplitude of 100V. This DC voltage is used as a feedback signal for AR2, thus reducing any modulator nonlinearity to a very low value and assuring an RF voltage strictly proportional to the generated saw tooth voltage.

An additional current can be applied to the summing junction of AR2 by means of the LOW LEVEL ADJ. potentiometer. This control can be used for the manual sweep of the RF voltage or for adjusting the starting point of the sweep. The LOW LEVEL ADJUST, in conjunction with the HIGH LEVEL ADJUST is normally used for the limited scan of any portion of the spectrum.

A DC voltage proportional to the RF signal is also applied to AR3 by means of the DC/AC ratio control. When relay K1 is de-energized, AR3 is used as a precision DC amplifier. With K1 energized, amplifier AR3 becomes an integrator which produces a linear down scan of the DC voltage. The down scan speed is adjustable over essentially the same range as the up scan speed. Amplifier AR4 is a precision DC inverter. Either a positive or negative DC voltage proportional to the AC voltage can be selected by the "DC POL" switch and be applied to the low end of the RF coil for the analysis of negative or positive ions in the mass spectrometer. The maximum value of the DC voltage is about 100 volt.

Amplifier AR5 is a precision level detector adjustable to any point of the sweep range by means of the "TRIG LEVEL" control. It is used to trigger either the sweep generator reset (thus automatically starting a new cycle), or the DC down scan (which in turn resets the sweep at the end of the cycle to maintain automatic operation).

RF unit

Refer to schematic, Figure 12.

Q1 is a crystal-controlled, 1.8 MC oscillator using an FET transistor and a parallel resonant quartz crystal. The oscillator output is applied to Q2 which is connected as a modulated amplifier. The emitter follower Q3 provides a low impedance drive for the power amplifier Q4. The low impedance of the emitter follower Q3 and modulation of both the voltage amplifier Q2 and power amplifier Q4 permits stable operation over the very wide dynamic range (2V to 1800V p-p) without the need for neutralization.

For the proper operation of the monopole filter it is of great importance that the power supply produce an undistorted sine wave AC voltage. Harmonic distortions do not only change the peak heights and shapes but also the mass scale. These effects depend on the relative phase angles and are, therefore, strongly dependent on the position of the

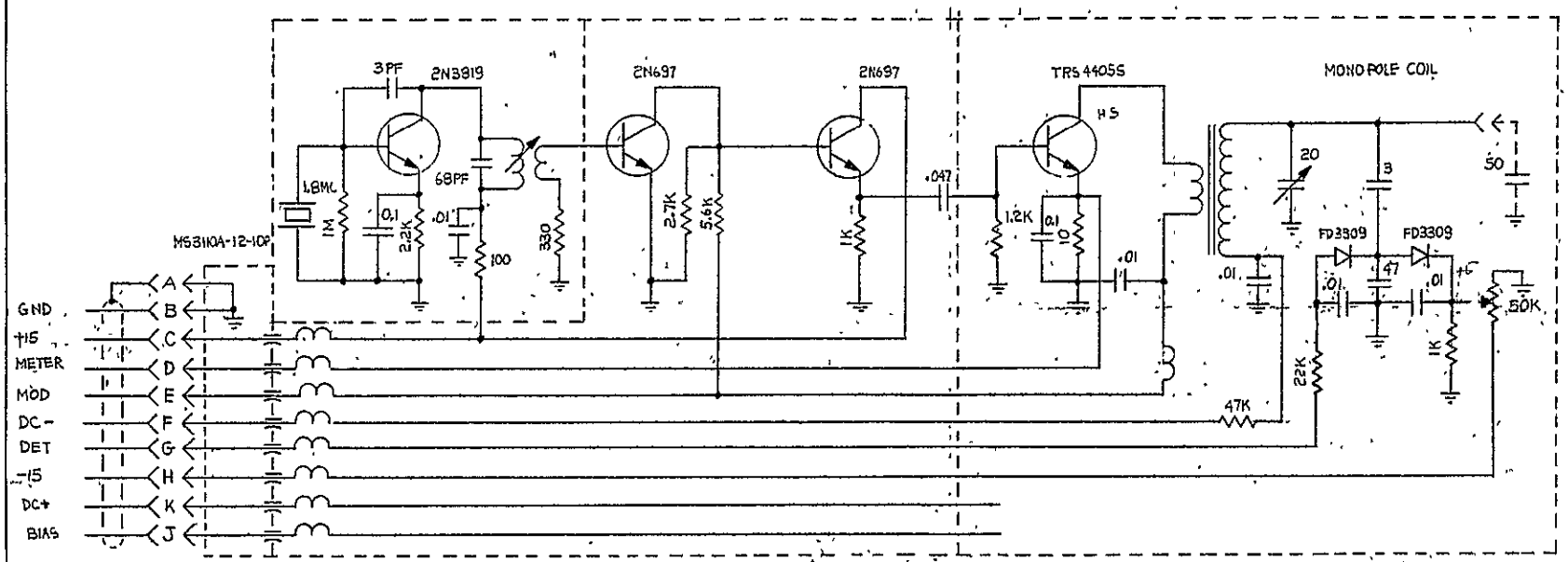

QTY REQD	PART NO	DESCRIPTION	SPECIFICATION	ITEM NO.

LIST OF MATERIAL

UNLESS OTHERWISE SPECIFIED
ALL DIM ARE IN INCHES
TOLERANCES
X= 06 XX= 02 .XXX=.005
ANGLES
MACHINE FINISH ✓
BREAK SHARP EDGES AND COR .005 TO .020R APPROX

MATERIAL

	DR	DATE
	J.D'A FEB-27	
	CHK	JUN-6-67

APPROVALS

RELEASED

FINAL FINISH

NEXT ASSY	USED ON
APPLICATION	

GCA TECHNOLOGY DIVISION
Bedford, Massachusetts
GCA CORPORATION

TITLE

Figure 12. Power supply RF unit.

SIZE	DRAWING NO.	REV
C	1-236-200	

SCALE | WT | SHEET 30F 31

DO NOT SCALE

43

tuning capacitor. An adjustment for minimum emitter current results in better mass spectra than an adjustment for maximum AC voltage. Besides the intended slow change of amplitude during a mass scan, there should be no other modulation of amplitude or frequency since this would have a strong effect on the peak shape. These clean output conditions must be maintained over the whole wide range of output voltages. Occasionally, wild oscillations have been observed over a limited voltage range which resulted in complete suppression of the corresponding mass peaks. Careful layout of the wiring and shielding between the RF stages have eliminated these difficulties.

G. Comparison of the Experimental Observations With Theoretical Expectations

This comparison is quite important because the extremely complex phenomena in a monopole mass spectrometer necessitate far reaching simplifications in the theoretical treatment. Nevertheless, it will be shown that the general behavior of the monopole instrument is surprisingly well described by the simple formulae previously developed. Some of the more special experimental results have been already mentioned at the related places in the previous theoretical chapters. The following sections are dedicated to the most important properties of the instrument as there are, dispersion, mass scale, peak shape, resolution, sensitivity, high pressure operation and finally the design criteria for the best choice of basic instrument parameters.

Mass scale and dispersion.- The normal mass scan of a monopole mass spectrometer is performed by increasing both, the DC voltage U and the AC voltage V in proportion to each other, thus keeping the voltage ratio $R = U/V$ constant. If the ion accelerating voltage is kept below about 10 volt, then all ions, except hydrogen, require at least 20 RF cycles to pass the field. In this case, the mass scale is essentially linear and given by Equation (24) previously developed.

$$U_o = U^* R^2 M \tag{24}$$

The constant U^* can be calculated either theoretically from Equation (4) by use of the basic system parameters ω and r_o or from experimental results by measuring U_o and V_o for a known mass number M and by using Equation (24).

The parameters of the laboratory model are:

$$\nu = 1.8 \times 10^6 \text{ cps}$$

$$r_o = 0.3'' = 0.762 \text{ cm}$$

which results in

$$U^*_{\text{theoretical}} = 77 \text{ volt}$$

The argon peak M = 40 was observed at U_o = 64 volt and V_o = 474 volt which results in R = 0.135 and

$$U^*_{experimental} = 88 \text{ volt}$$

Considering the great difficulty to accurately measure r_o and V, we find that $U^*_{experimental}$ and $U^*_{theoretical}$ are in fair agreement.

The dispersion of the monopole mass spectrometer is the voltage difference for adjacent masses and given by U^*R^2. The maximum value of R is R = 0.167 because of the stability limitation in the x-direction. Therefore, the maximum dispersion depends only on U^* which is proportional to ν^2 and r_o^2. The dispersion quadruples if either the frequency or the field radius is doubled. Unfortunately, in order to cover the same mass range, it is necessary to provide four times larger voltages. Considering also the increased dielectric losses at the higher frequencies one finds that an instrument of twice the size or twice the frequency requires at least 32 times more power to operate. The larger instrument has 4 times more sensitivity because the diameter of the entrance- and exit-aperture can also be doubled. However, the power consumption for this improved sensitivity soon becomes prohibitively high especially if heavier masses should be measured. This situation is even worse for a quadrupole mass spectrometer which requires four times this power since four rods have to be supplied. The quadrupole mass spectrometer has to be operated always with R ≈ 0.167 in order to obtain adequate resolution. In contrast, the monopole mass spectrometer can be operated with much smaller values of R which results in a very substantial saving in the power consumption. This feature of the monopole mass spectrometer is particularly valuable for space applications.

If the ion energy is increased, all peaks are shifted from the position U_o to $U_o + \Delta U$ where ΔU can be calculated from Equation (54) which can be written in the form

$$\Delta U = E\ (\beta N)^2 (\pi\alpha_o)^2 / (1 + \Delta U/U_o) \qquad (59)$$

We have seen previously that a peak occurs for $(\beta N)^2 = 0.8$ if $N \geq 10$ and if a medium size exit aperture is used. For the laboratory model we obtain L = 22.2 cm, r_o = 0.762 cm, α_o = 0.0343 and $(\beta N)^2(\pi\alpha_o)^2 = 0.0093 \approx 0.01$. We can neglect the last term in Equation (59) as long as $U_o \gg \Delta U$. In this case one obtains for the laboratory model $\Delta U = 0.01$ E. This shift is the same for all masses and, therefore, does not disturb the linearity of the mass scale. For instance the M = 40 peak previously mentioned and observed at U_o = 64 volt for a very small energy would be shifted by 0.8 volt to the new position, 64.8 volt, if the ion energy is increased to 80 volt. This means that the zero point of the whole mass scale is now offset by 0.8 volt. In this case, it was well justified to neglect the last term in

Equation (59) which amounts to only 1 percent. However, at the low end of the mass scale, this would no longer be true. For M = 1, U_o is only 1.6 volt, and $\Delta U/U_o = 0.5$. Therefore, the shift of the atomic hydrogen peak is less than for the molecular hydrogen peak and the shift of this latter one is less than the shift for the heavier mass peaks. This results in a slightly larger dispersion between H_1 and H_2 than between adjacent heavier masses. Under normal operating conditions, for E = 25 volt and R = 0.135 this effect is still quite small and not disturbing, since it effects practically only the H_1 and H_2 peaks. The dispersion between the hydrogen peaks is about 1 percent larger than between heavier adjacent masses. However, this effect can become quite noticeable if the ion energy is increased to 80 volt and the voltage ratio is reduced to 0.060. Under these conditions the dispersion between the hydrogen peaks is about 20 percent larger than for heavier masses. On a proportional mass scale starting with zero volt, the hydrogen peaks appear to be shifted to slightly higher masses. On a linear mass scale, exprapolated down from heavier masses, the hydrogen peaks appear to be shifted to lower masses. However, the peak width at half height is almost one atomic mass unit which is not enough resolution for most applications. Therefore, the instrument is normally not operated with such a high ion energy and low voltage ratio.

Great effort has been made to verify experimentally the theoretical shift of the mass scale as a function of the ion energy. The formulae which have been developed here could be well confirmed.

We have seen previously that the mass scale for very low ion energies should be practically linear. The observed deviations from linearity are much greater than theoretically expected and could be traced to a non-linear characteristic of the diodes and transistors used in the power supply. Special selections of the diodes and the application of compensating voltages have considerably improved the linearity. However, it is felt that more improvements in this regard are still possible and desirable. Nevertheless, the mass scale is sufficiently linear to permit easy determination of the mass numbers. This feature has been found to be extremely convenient in comparison to magnetic mass spectrometers. Especially the lack of any hysteresis effect and the accurate reproducibility of the peaks are very valuable.

Scanning methods and extended mass range.- Several methods of scanning the mass scale are possible. In the first prototype instrument, as described by Ulf von Zahn (Ref. 1), the DC and AC voltages were kept constant and the frequency was changed. In this case the mass is inversely proportional to the square of the frequency. A wide mass range, for instance mass 1-400, can be covered with a much smaller frequency range, for instance 20-1. However, the resolution ($M/\Delta M$) of such an instrument is constant, which is a disadvantage for fast recording, since peaks at the low mass end are too sharp to prevent clipping and peaks at the high mass end are not sufficiently resolved.

Another method of scanning has been described by R. E. Grande, R. L. Watters and J. B. Hudson (Ref. 9). In this case the frequency is

kept constant and the DC and AC voltages are increased proportionally; the mass is essentially a linear function of the applied voltages. In contrast to a quadrupole, the resolution of a monopole of finite length is proportional to the mass if the ion energy is kept constant. This means that the peak width stays essentially constant over the whole mass range and unit resolution can be obtained for all masses. The power supply for such an instrument is much simpler since the frequency is kept constant and tuning has to be performed only once. Unfortunately, rather high voltages are still required if very high masses shall be detected. It is the unique feature of the monopole over the quadrupole filter that this drawback can be partially removed by drastically reducing the DC to AC voltage ratio. This involves either a reduction of the resolution over the whole mass range, if the ion energy is kept constant, or a reduction of sensitivity, if the ion energy also is reduced. In both cases, the mass range is still limited by the maximum AC voltage delivered by the power supply and the existence of masses above this limit cannot be detected.

In order to avoid this limitation of the mass range and to maintain the highest sensitivity and resolution possible with a given power supply, a new type of mass scan (Ref. 10) has been tested, consisting of two parts:

(1) The low mass range is swept in the conventional manner by increasing the AC voltage and keeping the DC to AC voltage ratio constant. This ratio shall be rather high and close to the stability limit, in order to obtain good resolution even for rather high ion energies which are desirable to obtain good sensitivity. The highest mass which can be measured in this way depends primarily on the maximum AC voltage produced by the power supply.

(2) The adjacent higher mass range is then swept by reducing the DC voltage and keeping the AC voltage constant at its maximum value. The mass scale is again given by Equation (24), if $V_o = V_{max}$ = constant. The mass is inversely proportional to the DC voltage U_o.

$$M = (V_{max}^2/U^*)/U_o \qquad (24a)$$

In this regard the mass scale is identical to the one obtained in a conventional magnetic mass spectrometer if the magnetic field strength is kept constant and the scanning is performed with the acceleration voltage E. Figures 13 and 14 demonstrate the similarity with the mass spectrum of perfluorodimethylcyclohexane (C_8F_{16}). The upper spectrum, Figure 13, has been obtained with a monopole mass spectrometer by use of the novel scanning method. Figure 14, below, shows, for comparison, the same spectrum obtained with a small magnetic vacuum analyzer. It is obvious

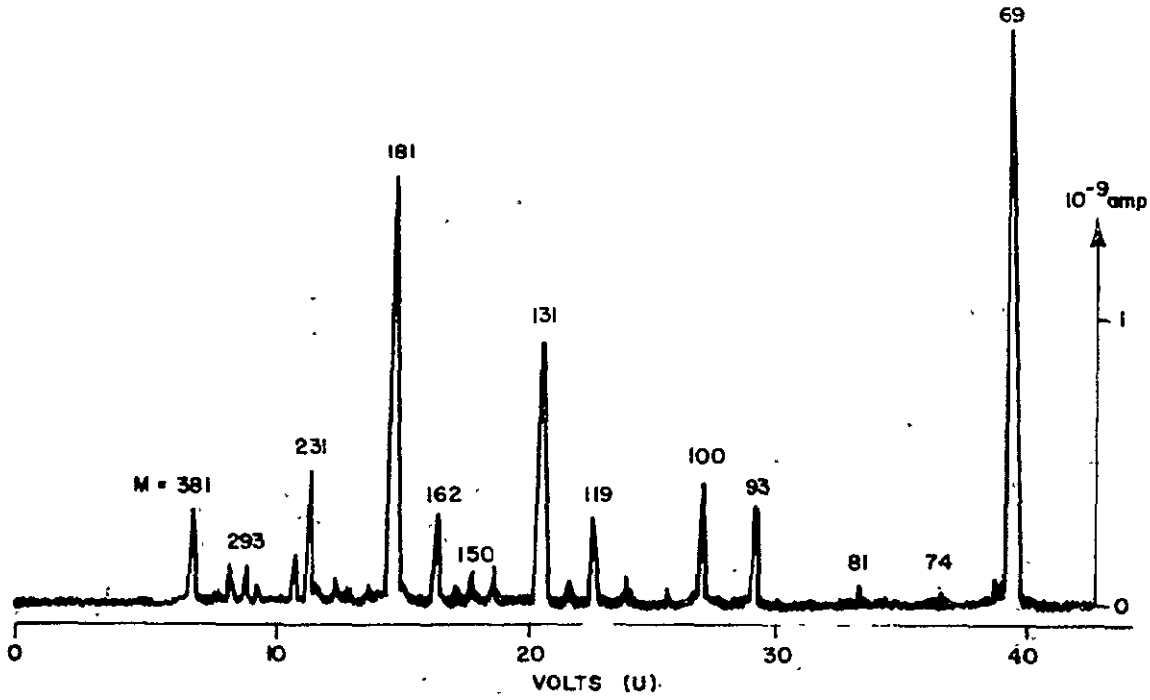

Figure 13. C_8F_6 with monopole.

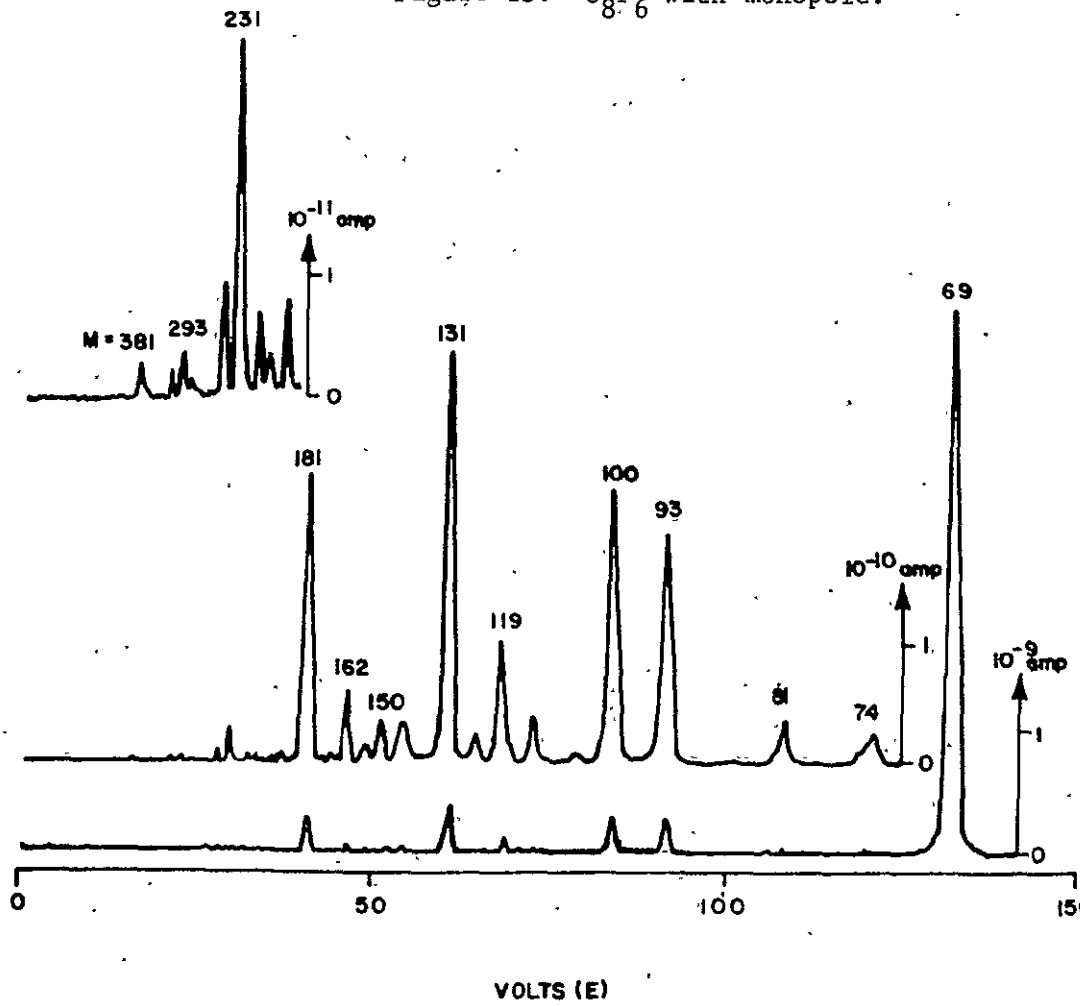

Figure 14. C_8F_6 magnetic.

that the monopole mass spectrometer provides much better transmission and sensitivity for high masses. In this regard it is similar to a magnetic mass spectrometer with magnetic sweep, since the acceleration voltage E is kept constant in both instruments. The experimental mass scale is in close agreement with Equation (24A) (see Figure 15).

The mass resolution $M/\Delta M$ increases proportionally with the mass number M during the regular scan over the low mass range, as will be discussed later in more detail, and decreases inversely proportionally to M during the new scan over the extended mass range. This results in a constant peak width ΔU for all masses which permits the use of the fastest constant sweep rate which is compatible with the electrometer-recorder system. No sudden change of the resolution occurs at the transition point between the low and the extended mass range.

The main purpose of the extended mass range is to detect with high sensitivity the presence of any ions which are beyond the regular mass range and to permit at least a rough determination of their masses. Since there is no upper limit of the extended mass range, no ions, regardless how heavy, can escape detection. This feature is especially valuable for vacuum analyzers in oil pumped systems where hydrocarbons with masses up to 463 might be present. Fortunately, this additional information can be obtained without increase of the power consumption. Only a moderate increase of scanning time is necessary. However, if an accurate mass analysis is mandatory, the regular mass range would be preferable because of the better resolution. Unfortunately, in order to extend the regular mass range from mass 48 to mass 381, it would be necessary to increase the AC voltage from V = 478 to 3800 volts. The power consumption would be at least 64 times larger and the minimum scanning time would be four times longer.

One valuable feature of the monopole mass spectrometer is the possibility to trade off sensitivity for resolution simply by reducing the energy of the ions. For applications where resolution is more important than sensitivity, it is possible to increase the resolution during the extended mass range by reducing simultaneously the ion energy. Scanning the ion energy is not critical since it has very little effect on the position of the peaks. If the ion energy E is reduced proportionally to U, the resolution stays constant over the extended mass range and the performance of the monopole mass spectrometer becomes quite similar to a magnetic spectrometer with electric scan. Even in this case, no increase of the power consumption is required, but the maximum scanning speed has to be slightly reduced in proportion to the smaller width of the peaks.

Peak width and peak shape.- A large number of measurements have been performed to study the peak width at half height ($\Delta U_{1/2}$) as a function of the operating parameters. According to Equation (55), $\Delta U_{1/2}$ should be proportional to E and independent of M and R. These facts could be well verified experimentally for mass 40 and 20 and for E = 15, 25 and 90 volt

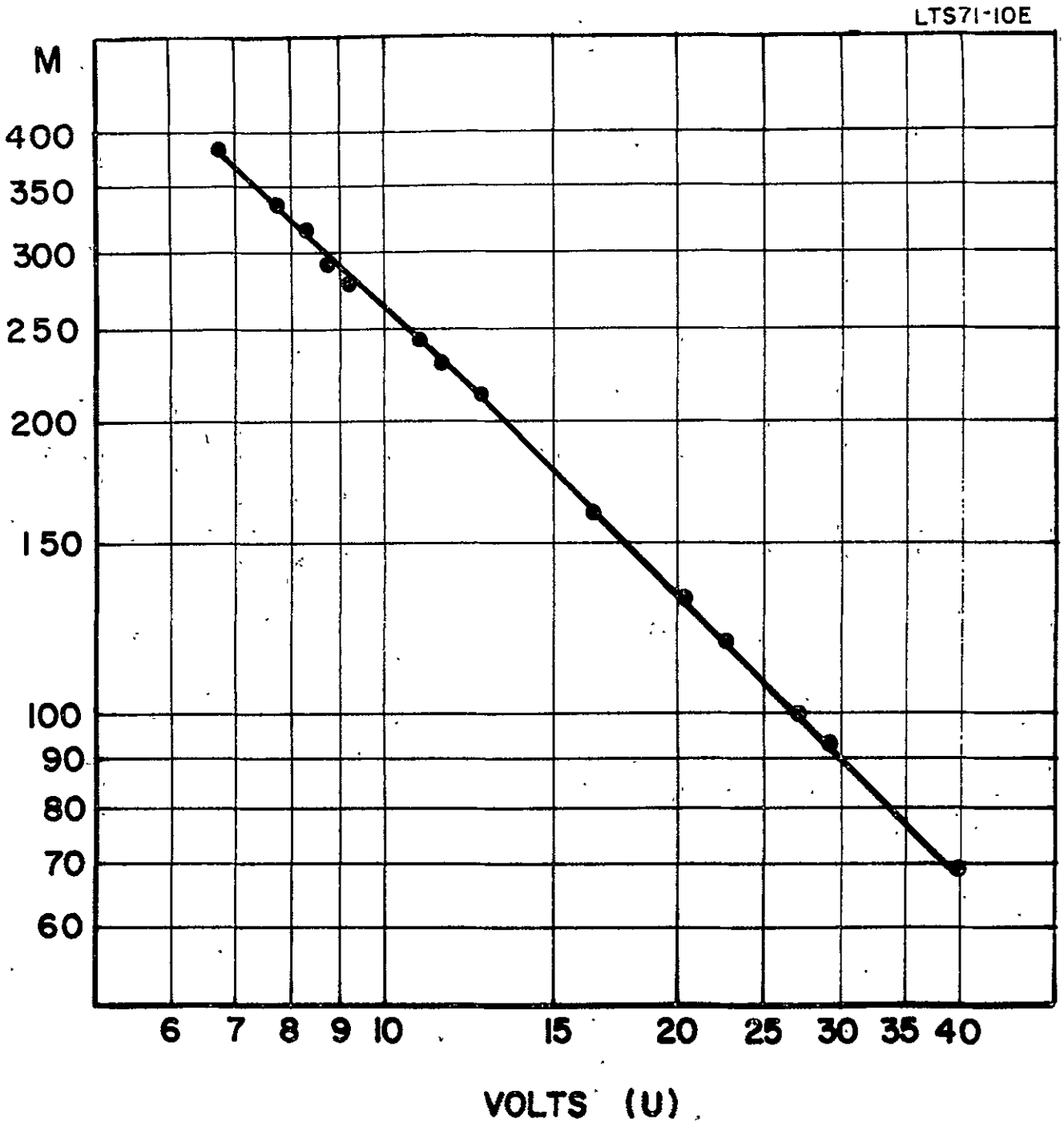

Figure 15. Mass scale of extended range.

and for R = 0.042, 0.080, 0.116, and 0.158. In all cases it was found that $\Delta U_{1/2} = 0.048\ E$. Since for the laboratory model $\alpha_o = r_o/L = 0.762/22.2 = 0.0338$ one obtains from Equation (55): $(\beta N)^2_{experimental} = 0.4$. This value is in close agreement with the one obtained previously. The following experimental formula can replace Equation (55).

$$\Delta U_{1/2} = 0.4\ (\pi\alpha_o)^2 E \qquad (60)$$

The dependence from α_o could not be checked since this would have required testing many monopole structures of different lengths and diameters. The factor 0.4 in Equation (60) depends only slightly on the size of the entrance and exit aperture and was obtained with a round entrance aperture of 0.047 inch diameter, sufficiently offset from the apex of the V-electrode in order not to be obstructed, and a triangular exit aperture of 0.08 inch height. The peak width at half height is very little effected by the size of these apertures. However, the peak tails are increased if the apertures are increased above the values mentioned above. On the other side, a reduction of the size of these apertures results in a severe loss of sensitivity. The dimensions given represent a good compromise for good resolution and sensitivity and have been used for most of the measurements.

The normal peak shape is triangular with a sharp top, the upper part with practically straight slopes. The tails of the peaks extend over several mass numbers and the one on the side of higher mass numbers is more intense. For this investigation argon has been admitted to the instrument to a pressure of 3×10^{-4} torr. The 40 peak has been recorded with a linear electrometer with different multiplier voltages. The following table shows the width of the 40 peak at different relative heights:

Table 2

EXPERIMENTAL PEAK SHAPE

At 0.5 of peak height	M = 39.95 - 40.0	ΔM = 0.15
0.1	39.9 - 40.5	0.6
0.05	39.9 - 40.7	0.8
10^{-2}	39.9 - 41	1.1
10^{-3}	39.5 - 42	2.5
10^{-4}	39 - 44	5
10^{-5}	37 - 46	9

The interference with the adjacent mass 39 is 10^{-4} and with 41 is 10^{-2}. Outside mass 36 to 48 interference becomes negligible which should

permit there the detection of trace impurities in the part per million range. Scanning was performed extremely slow from low to high mass numbers to provide sufficient recovery time for the electrometer. Nevertheless, it is possible that part of the longer tail at higher masses was caused by overloading of the electrometer. Therefore the figures given above represent the upper limit of the peak width.

Flat topped peaks are more desirable for accurate intensity measurements especially if the mass spectrum is scanned by stepping from peak to peak. Requirements for reproducibility and stability are much less stringent. Flat topped peaks have been achieved with magnetic mass spectrometers if the exit slit is wider than the image of the entrance slit, or with quadrupole mass spectrometers if a very wide exit aperture and a very narrow entrance aperture is used. With both instruments this results in reduced resolution and sensitivity which have to be tolerated to achieve the flat peak tops.

With monopole mass spectrometers it is probably also possible to achieve flat topped peaks by the same method. However, since 3/4 of the exit aperture of the equivalent quadrupole structure are blocked by the V-electrode, the requirements on the narrow collimation of the incoming beam are more severe. It will also be of advantage to use a short and wide monopole structure with a large form factor α_o. No attempts have been made to verify these assumptions since there are more simple ways to achieve the same goal.

For instance, a modulation of the DC scanning voltage U with a small superimposed AC voltage of about 1000 cps results in wider peak tops, their width being proportional to this AC voltage. The frequency must be above the electrometer response in order to obtain average output signals. The peak shape depends on the waveform of the AC voltage: A sine wave produces a concave peak with slightly higher edges, a triangular wave produces a convex peak. Both shapes have been verified experimentally. With a combination of sine and triangular wave it should be possible to obtain practically flat peaks.

In order to obtain the same peak widening for all masses it is necessary to change the amplitude of the modulation voltage with the scan voltage. This can be avoided if both the DC and AC voltages are modulated, thus keeping their ratio R constant. This has not been tested yet since it would have required major modifications in the power supply.

Another possibility is the modulation of the ion energy. Since this shifts the whole mass scale, all peaks are widened by the same amount. However, because of the sensitivity variations discussed previously the peak tops will not be perfectly flat and slightly different for each peak. This could be used to eliminate the effect of the sensitivity variations.

In all these cases, peak widening results in a reduction of peak height such that the area of the peak stays practically constant. It

is an advantage of these methods to permit external adjustment of this trade off without need to exchange the entrance aperture.

Another possibility to obtain flat peaks is with a peak seeking device, similar to the one used by General Electric in their magnetic vacuum analyzer. This device works well on large peaks if the gain is well adjusted. More development is necessary to adopt this method for scanning of the whole mass spectrum.

Resolution and peak separation.- The resolution is defined as the ratio $M/\Delta M$ where ΔM is the peak width measured in mass units at a given fraction of the maximum peak height. For this fraction the values 50, 10, 5 and 1 percent are commonly used. We will use 50 percent or half height resolution to permit comparison with published data. One obtains from Equations (60), (4), and (31)

$$M/\Delta M = U_o/\Delta U = U^* R^2 M/(0.4\pi^2 \alpha_o^2 E) = 20\, R^2 N^2$$

One sees that the resolution depends only on the voltage ratio R and on the number N of RF cycles needed to pass the field

$$N = (0.22/R)\sqrt{M/\Delta M} \qquad (61)$$

For R = 0.167, corresponding to the top of the stability diagram, the factor $0.22/R = 1.32$ compares favorably with von Zahn's (Ref. 1) value 1.5 and Dawson and Whetten's (Ref. 3) value 1.2.

Equation (61) is more general since it can also be used for lower R values. In this case the resolution decreases rapidly since it is proportional to R^2.

If all ions are accelerated by the same voltage E, then N is proportional to $\sqrt{M}$ and $M/\Delta M$ is proportional to M. Therefore, the peak separation stays constant over the whole mass range and describes better the performance of a monopole mass spectrometer than the mass dependent resolution. The peak width at half height expressed in atomic mass units can be obtained from Equations (60) and (24):

$$\Delta M_{50\%} = 0.4\pi^2 \alpha_o^2 E/(U^* R^2) \qquad (62)$$

or at 5% height:

$$\Delta M_{5\%} = 2\pi^2 \alpha_o^2 \, E/(U^* R^2) \tag{62A}$$

Two adjacent peaks of equal height are for most applications adequately resolved if they are separated by a 10 percent valley, corresponding to $\Delta M_{5\%} = 1$. The maximum permissible energy E_{max} is given by:

$$E_{max} = \Delta M_{5\%} \, R^2 U^* / (2 \pi^2 \alpha_o^2) = \Delta M_{5\%} \, R^2 \, 600 \, \nu^2 L^2 (m_1/e) \tag{63}$$

which is in good agreement with the experimental results. It should be noticed that E_{max} does not depend on the field radius r_o nor on the mass number M. The ion energy E should be kept above about 10 volts, preferably to about 100 volt in order to minimize charge up effects. This limits the minimum length and frequency product which can be used to

$$\nu L > \sqrt{\frac{E_{max}/\Delta M_{5\%}}{600 \, (m_1/e)}} \Big/ R \tag{64}$$

For example, for $E_{max} = 10$ volt and $R = 0.15$ one obtains

$$\nu L > 12 \times 10^6$$

However, if possible, it would be better to use a larger product, perhaps about 30×10^6.

Sensitivity.- Absolute sensitivity measurements are difficult to perform since they depend on the multiplier gain. This gain measurement is not reliable since the first dynode must be near ground potential if the total ion current is measured but is at high voltage during normal operation of the multiplier. This change of the field conditions may change the number of ions that strike the first dynode.

However, numerous relative sensitivity measurements have been made to study the sensitivity dependence on the size of the entrance and exit apertures, the ion energy and the voltage ratio. The following results have been experimentally found.

1. Entrance and Exit Apertures

If the triangular height of the entrance aperture h_1 and of the exit aperture h_2 is very small compared to r_o then the sensitivity is

proportional to $h_1^2 h_2^2$. For larger apertures the increase is slower (see Figure 16) and above $h_1/r_o = 0.2$ and $h_2/r_o = 0.2$ there is practically no further increase of sensitivity. This indicates that now the monopole rod limits the beam acceptance. Further increase of the sensitivity requires a larger instrument where h_1, h_2 and L are increased in proportion to r_o. In this case the sensitivity is proportional to r_o^2 as long as the ion beam completely fills the entrance aperture.

2. Voltage Ratio

It has been found experimentally that the sensitivity is roughly proportional to $\sqrt{0.167 - R^2}$. If R = 0.167, corresponding to the top of the stability diagram, the sensitivity becomes zero. For smaller values of R the sensitivity increases first rapidly and later more slowly. About half of the maximum sensitivity is reached for R = 0.126.

3. Ion Energy

The effect of the ion energy is more difficult to study because it is partly caused by the ion source and partly by the monopole. Increase of the energy reduces the angular spread of the beam and increases the transmission of the monopole as long as the beamspread is larger than the acceptance angle of the monopole. This results in an increase in sensitivity with an increase of energy up to about 20 volt and constant sensitivity for higher voltages. The transition point depends on the geometry of the ion source and the monopole. In addition, ions with smaller energies are more suppressed by charge up effects which can never be completely eliminated. Superimposed upon these major effects are the small sensitivity variations as a function of energy which have been discussed earlier and which further complicate the experimental investigation of the sensitivity-energy relations. Herzog (Ref. 11) has measured variations of the N_2/O_2 peak height ratio in air as a function of ion energy and found fair agreement with the theory.

Let us assume that separation of adjacent peaks is required and that Equation (63) has to be fulfilled. In this case E and R are interrelated; small values of R require very small values of E which reduces the sensitivity. On the other end, large values of R result also in reduced sensitivity. In between is a broad sensitivity maximum between R = 0.1 - 0.15 and E = 40 - 100 volt. These ion energies are much larger than those usually used with quadrupole instruments. Therefore, a wider energy spread can be tolerated which is an important advantage of the monopole instruments.

4. Geometry Effects

The effect of the field length L and radius r_o could not be checked experimentally since there was only one instrument available. Therefore, these effects have to be concluded from theoretical considerations.

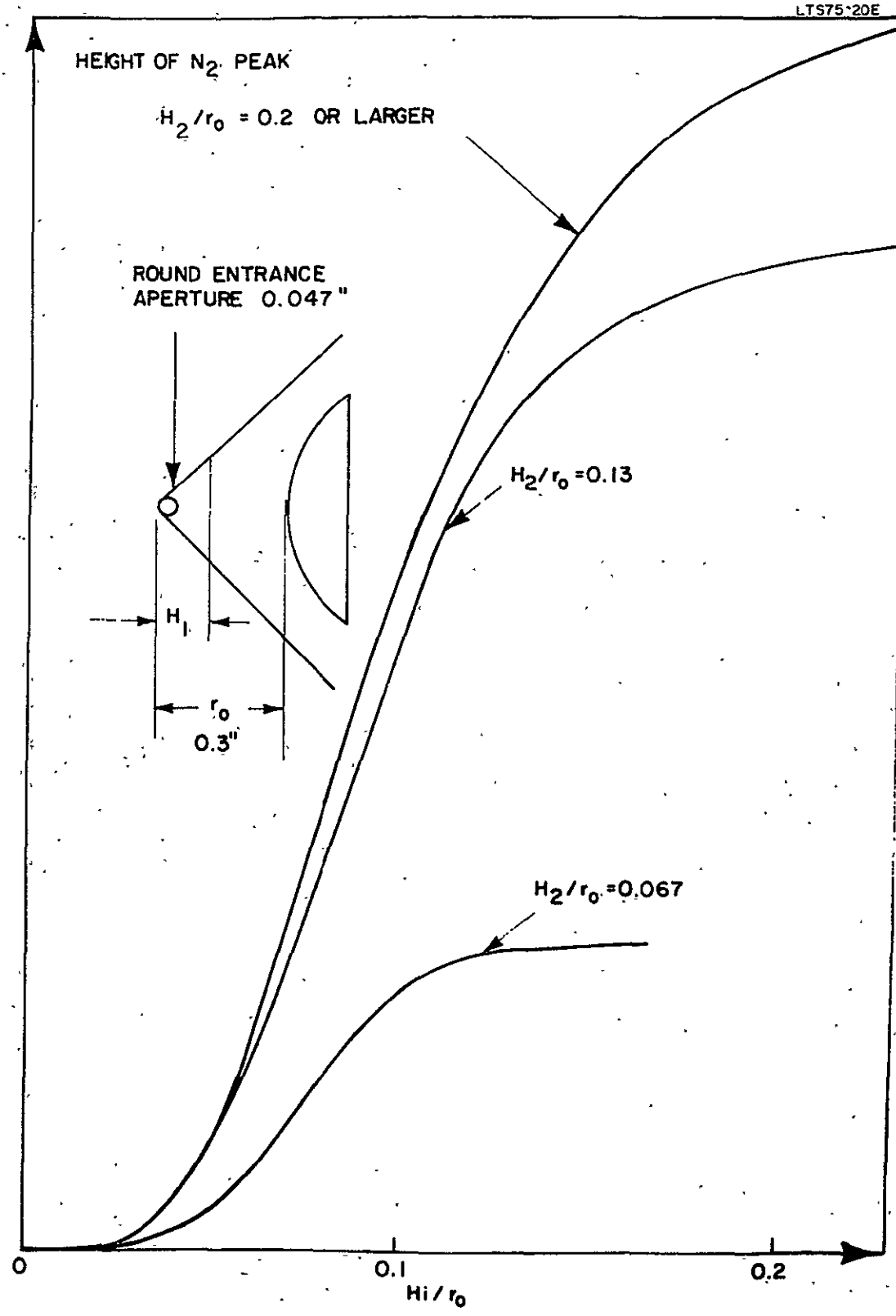

Figure 16. Sensitivity as a function of apertures.

The maximum acceptance angle is proportional to the field form factor α_o and the sensitivity is proportional to α_o^2. As we have seen earlier, the sensitivity is also proportional to r_o^2. Therefore, the combined effect due to beam spread and beam width is that the sensitivity is proportional to r_o^4/L^2. Assuming that h_1, h_2, R and E have already been optimized as discussed above, then the only way to improve the sensitivity is to make the instrument wider and shorter. The consequences will be discussed in the next section.

Trade-off between the basic system parameters and their optimum choice.- In this section the voltage and power requirements of a monopole mass spectrometer will be discussed.

The capacitance of the rod to ground is proportional to L and independent from r_o, if the diameter of the housing is also increased proportionally. Therefore, C/L is a constant. In order to maintain the same peak separation it is necessary to keep the product νL = constant (see Equation (64)). Therefore, the capacitive reactance of the rod is independent of L and r_o. The power consumption P is given by

$$P = (V/\sqrt{2})^2 \, 2\pi\nu \, C/Q$$

where Q represents the quality factor of the RF circuit. At frequencies around 10^6 cps most of the losses occur in the resistance of the coil which shall be called ρ. Compared to these losses dielectric and radiation losses are negligible. In this case we obtain

$$1/Q = 2\pi\nu \, C \, \rho$$

If one uses the same coil for monopoles of different dimensions then ρ is a constant and P becomes

$$P = 2\pi^2 \, (C/L)^2 \, \rho \, V^2\nu^2L^2 \tag{65}$$

By use of Equations (4), (23) and (24) we obtain

$$P = \frac{\pi^2(C/L)^2\rho}{300(m_1/e)} \, U^{*2} \, E_{max} \, M^2/\Delta M_{5\%} \tag{66}$$

The power consumption is proportional to the required resolution $M/\Delta M$ and to the maximum mass M and energy E_{max} of the ions to be analyzed.

It does not depend on the voltage ratio R. C/L is a constant, about 2 pF/cm, and smallest if the housing is far away from the rod. Naturally, the coil resistance ρ should be as small as is practically feasible. But, most important, U^* should be small, which is also desirable to avoid high voltage breakdown of the insulators. Since U^* is proportional to $\nu^2 r_o^2$, P becomes proportional to $\nu^4 r_o^4$.

The following table compares five typical cases, all with the same peak separation $\Delta M_{5\%} = 1$ which requires that ν is inverse proportional to L. It was previously explained that the sensitivity S is proportional to r_o^4/L^2.

Table 3

DESIGN TRADE OFFS

Case	Field Radius	Field Length	Frequency	U^*	Power	Sensitivity
1	r_o	L	ν	U^*	P	S
2	$2r_o$	2L	$\nu/2$	U^*	P	4S
3	$2r_o$	L	ν	$4U^*$	16P	16S
4	r_o	L/2	2ν	$4U^*$	16P	4S
5	$2r_o$	4L	$\nu/4$	$U^*/4$	P/16	S
6	$r_o/2$	L/4	4ν	$4U^*$	16P	S

This table shows the effect of r_o and L on P and S. If the instrument is enlarged in proportion P stays constant and S is increased (case 2). If only r_o is increased or L reduced then S is also increased but the increased power requirement makes this increase of the sensitivity rather costly (cases 3 and 4). One obtains a better increase of sensitivity for the same amount of additional power if r_o is increased than if L is reduced. A larger and much longer instrument (case 5) provides the same sensitivity but can be operated with much less power. On the other side, a smaller instrument requires much more power to obtain the same sensitivity (case 6).

The following conclusions can be drawn:

(1) It is in general an advantage to make the monopole as long as the available space allows despite the reduced sensitivity. The greater length permits operation with lower frequencies for the same resolution which results in smaller voltages and much smaller power consumption. The

only exception to this rule is an application where the instrument has to be operated at a relatively high pressure where the mean free path limits the useful length of the monopole.

(2) The field radius should be made as large as possible and compatible with the available power. This limitation is quite strong since a small increase of the field radius requires a very large increase of the power (case 3). The obtained sensitivity is proportional to the available power.

(3) After L, E_{max} and $\Delta M_{5\%}$ has been chosen ν can be calculated from Equation (64). A large value of R has to be chosen to keep ν small, since this has a very large effect on the power consumption. On the other hand, if R approaches 0.167 the sensitivity becomes zero. A good compromise is any value of R between 0.1 to 0.15.

$$\nu = \sqrt{(E_{max}/\Delta M_{5\%})/(600\ m_1/e)}\ /(RL) \tag{67}$$

(4) After the mass range M has been chosen one can calculate from the available power and Equation (66) the maximum permitted value of U^*.

$$U^{*2} = \frac{300(m_1/e)}{\pi^2 (C/L)^2 \rho}\ P/(E_{max}\ M^2/\Delta M_{5\%}) \tag{68}$$

Finally from Equation (4) one obtains r_o

$$r_o = (1/(2\pi\nu))\ \sqrt{U^*/(300\ m_1/e)} \tag{69}$$

One can see from the above that for all the desirable features, as there are high mass range M, high resolution $M/\Delta M$, high sensitivity S, and high permissible ion energy E_{max}, one has to pay either with the larger size of the instrument or with much higher power consumption. The choice between these alternatives depends on the particular application.

H. Effect on the Mass Spectra of a Relatively High Pressure in the Monopole Section

Such a situation can occur either if the instrument is used without a separate pump to analyze a mediocre vacuum or if the pressure is purposely raised to permit detection of impurities at very low relative concentrations.

If the pressure in the analyzer is increased until the mean free path λ becomes comparable to L then a fraction $\exp(-L/\lambda)$ of the ion beam entering the monopole field is lost due to scattering on the ambient gas. Therefore, the peak height is no longer proportional to the pressure but reaches a maximum if $\lambda = L$ and declines for higher pressures. For instance, for the laboratory instrument with L = 22.2 cm and for argon at 25°C this maximum corresponds to a pressure of 2.4×10^{-4} torr. At this pressure the peak height is reduced by the factor 0.37. The deviation from the linearity becomes already noticeable at a pressure of 2×10^{-5} torr. Nevertheless it is possible to operate the monopole at much higher pressures which are finally limited by a glow discharge in the monopole or in the multiplier. The instrument has been successfully operated with argon at a pressure of 2×10^{-3} torr. Neither the peak width nor the peak tails are increased at this high pressure which is an important advantage over magnetic vacuum analyzers. The monopole mass spectrometer is still quite useful at this pressure for a qualitative analysis if a sensitivity loss of about three orders of magnitude can be tolerated. Quantitative measurements can also be performed after proper calibration of the instrument. However, care is necessary for the interpretation of the spectra since each peak height corresponds to two different pressures. One has to correlate falling or rising total pressures with falling or rising peak heights to determine the appropriate part of the calibration curve.

Numerous calibration experiments have well confirmed the theoretical expectations. Only at pressures above one micron are the peak heights slightly larger than expected. Apparently some of the ions are scattered by a small angle only and focused back into the beam.

A small fraction of the scattered ions reach the multiplier and cause a background current which is independent of the mass. This background current is proportional to the square of the pressure because both the ion current and the scattering probability are proportional to the pressure. For instance, at an argon pressure of 2×10^{-4} torr this background current was 140 ppm of the 40 peak. Since this background current is rather constant, it is still possible to see superimposed peaks of about 10 ppm. Nevertheless, this background is quite disturbing for the detection of trace impurities since it prohibits the use of a high electrometer sensitivity or of the more sensitive pulse counting technique. It is expected that better shielding of the multiplier entrance aperture and differential pumping of the analyzer could significantly reduce this background and improve the capability to detect trace impurities in the part per million range.

I. Monopole Operation With Only a DC Voltage Applied to the Rod

If the AC voltage V is kept zero and the normal polarity of the DC voltage is used, all ions are attracted to the rod and practically

no ions can pass the filter. However, if the DC voltage is reversed, the monopole structure acts as a lens and focuses the beam in the y-direction. At the same time the beam is defocused in the x-direction. These lens effects are well known for quadrupole structures and have been utilized extensively in high energy particle physics.

The effect has been tested with the laboratory model monopole instrument. Argon ions with 20 electron volt energy have been used. If the rod and V-electrode are grounded, a very small ion current is detected with the multiplier. This current increases about 500 times if +0.24 volt are applied to the rod. Apparently the focusing force in the y-direction is by far more effective than the defocusing force in the x-direction. This experiment demonstrates also the great importance of having exactly the right voltages applied to the rod during a normal scan. If the voltage ratio R is not kept accurately constant, which is rather difficult for small voltages, then serious deviations from the right peak heights are possible. This may be one of the reasons why the H_1/H_2 ratio exhibits abnormally large variations.

For the calculation of the required DC voltage U, one can still use all previously developed equations by setting q = 0 and reversing the polarity of a. One obtains finally:

$$U = E\ (\pi\alpha_o)^2\ (\beta N)^2 \qquad (70)$$

This equation may first look strange since it contains N which is related to the AC field which is not present in this case. However, a closer inspection reveals that for q = 0 ... β becomes proportional to $\sqrt{a}$ which is inversely proportional to ν. Since N is always proportional to ν the product βN becomes independent of ν if q = 0. Actually the product $\pi\beta N$ is the phase angle of the major oscillations and has no direct relation to the AC field. It is affected only indirectly by the focusing action of the AC field. Equation (70) can also be obtained directly from the equation of motion by eliminating the term caused by the AC field; the result is the same.

If a wide parallel beam enters the field, it is focused for βN = 0.5. If the beam enters the field at y = 0 but in different directions, it is focused for βN = 1. If this diverging beam enters the field at slightly positive values of y, it is necessary that βN is slightly smaller than 1 in order to obtain maximum transmission. Experimentally the maximum transmitted intensity was found for βN = 0.9 in excellent agreement with the theory. It should be mentioned that Equation (70) does not contain M and only E. The monopole structure has no mass resolution, if operated only with DC voltages, but acts as an energy filter, which is in agreement with general principles of the ion optic. Application of the monopole or quadrupole structure as an energy filter may be of practical value if the beam axis should not be deflected.

J. Monopole Operation With Only an AC Voltage Applied to the Rod

This special case is of particular interest, since quadrupole filters have been operated in this manner. It was first shown by Paul and Steinwedel (Ref. 12) that in this case all masses above M are transmitted and all masses below M are filtered out if M is calculated from Equation (8) with q = 0.92. The observed signal is therefore the integral of a regular mass spectrum from $M_1 = \infty$ to M = M. This signal is essentially a step function and each step corresponds to one mass peak. If the AC voltage is reduced to a value corresponding to a mass slightly smaller than one, then all masses are transmitted and the signal represents the total ion current. In actuality the signal is a much more complicated function of the instrument parameters and not so simple to interpret.

The corresponding case for a monopole mass spectrometer has not been investigated so far. It will be shown below that for U = 0, a = 0 and R = 0 one still obtains a mass spectrum of very low resolution and with a square mass scale. One obtains from the previously developed equations:

$$V = E\ N\ .2\sqrt{2}\ (\pi\alpha_o)^2\ (\beta N) \qquad (71)$$

Experimentally, the argon 40 peak with ions of 88 electron volt energy, has been observed at V = 56 volt. This results in $\beta N \approx 1.0$, similar as in the preceding section. For the laboratory instrument one obtains

$$V = E\ N/30 = \text{prop.}\ \sqrt{EM} \qquad (72)$$

Since N is proportional to $\sqrt{M}$, the mass number becomes proportional to V^2. This mass scale has been well confirmed experimentally; it is compressed for higher mass numbers and therefore the resolution becomes very small. Peak 20 is only a small hump on the flank of peak 40. However peak 4 is well separated.

The significance of this special case comes from the fact that it represents the end point for the extended mass scan. At this point U_o becomes zero and the sensitivity drops down significantly for all masses larger than the one calculated from Equation (72). This represents the practical limit of the extended mass range. Fortunately, this limit is rather high, approximately M = 18,000 for E = 40 volt and V = 800 volt. One sees also that the mass scale is slightly different from the approximate Equation (24A): If U_o is zero the mass number is not infinite but only very large.

K. Negative Ions

The monopole mass spectrometer should also be useful for the detection of negative ions if a positive DC voltage is applied to the rod. Unfortunately negative ions of about 30 electron volt energy cannot enter the electron multiplier if it is operated in the normal way with the anode near ground potential and the first dynode at minus 3000 volt. For the detection of negative ions it is necessary to keep the first dynode at about +500 volt which results in an anode potential of about +3500 against ground.

The detection of extremely small currents on an electrode which is at such a high potential above ground results in considerable experimental difficulties which can be solved in different ways. The method which was successfully used here consisted of the following. A capacitor was used to separate the high voltage of the anode from the low voltage of the pulse amplifier input. In this case, the multiplier power supply must be perfectly free of any ripple and transients. The coupling condenser must be of very high quality and the whole circuit must be very well shielded in order to permit the use of the full gain of the pulse amplifier necessary for the detection of single ions. Pulses which are above an adjustable background level are used to trigger secondary pulses of uniform length and height. These pulses are measured with a logarithmic electrometer. This method of ion detection is preferable over the straight electrometer type measurement since it actually measures the count rate which is essentially independent of the multiplier voltage and gain. Therefore, the major error source of any multiplier current measurement can be eliminated.

A gas mixture consisting of sulphur hexafluoride and water vapor was introduced into the mass spectrometer and ionized in the conventional way by electron impact. Figure 17 shows the mass spectrum thus obtained. The following negative ions have been observed: large peaks of atomic and molecular hydrogen and smaller peaks of atomic oxygen, fluorine, SF_5 and SF_6. Occasionally a very small peak at mass 17, probably OH, has been observed.

At the beginning of these investigations, it was not certain that negative ions could be analyzed because electrons released from the rods and the exit slit by ion impact might contribute to a very large background current. The successful experiments have demonstrated conclusively that it is quite possible to obtain excellent spectra of negative ions with a monopole mass spectrometer.

This demonstration of the feasibility to study negative ions opens the possibility of investigating the negative ion composition of the upper atmosphere. The knowledge of the negative ion composition is still the missing link for a successful interpretation of the chemistry of the upper atmosphere.

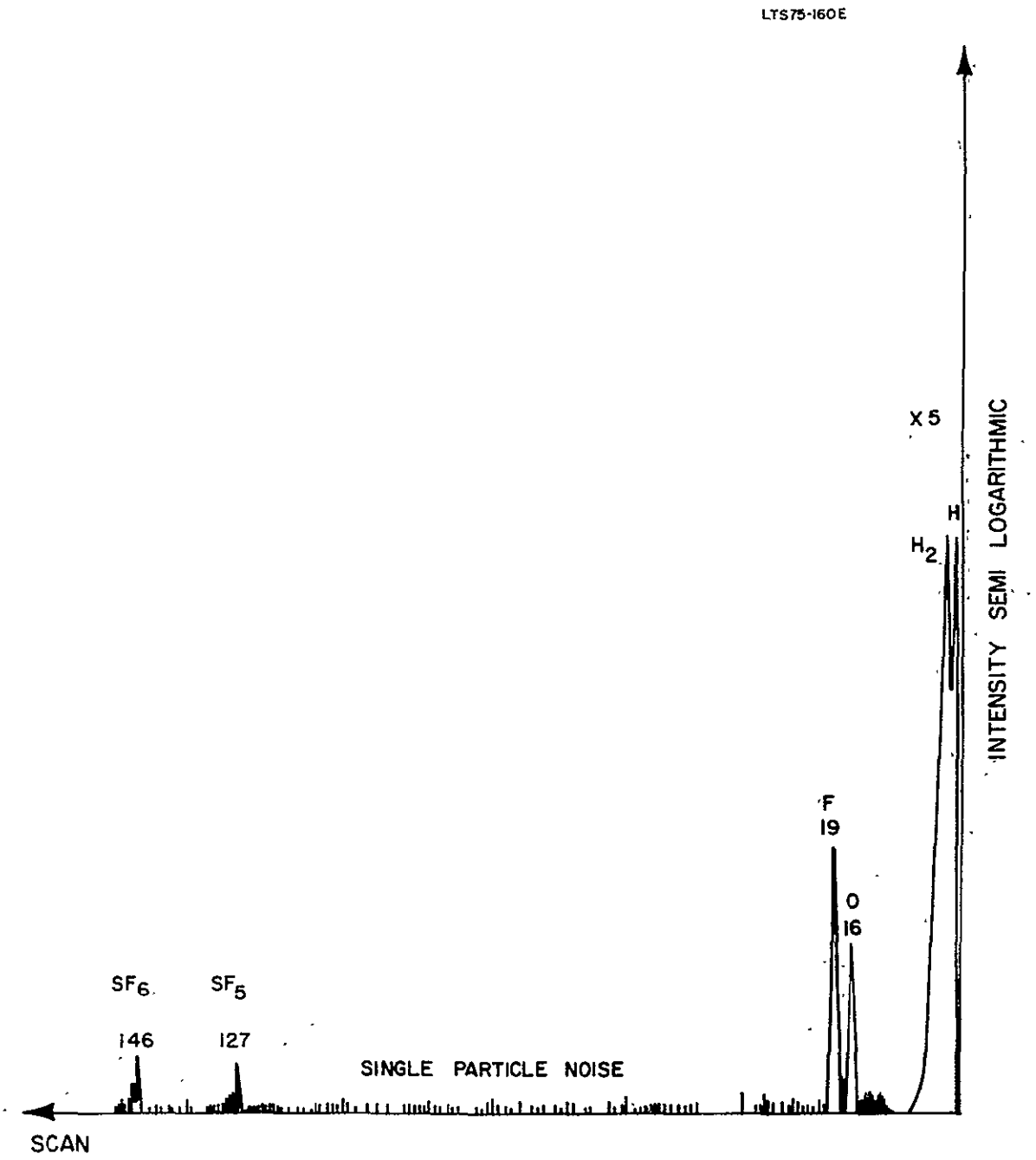

Figure 17. Negative ion spectrum of SF_6.

L. Fringe Field Effects

Between the entrance aperture and the rod electrode exists a strong electric field which has been neglected so far. This field changes significantly the energy of the incoming ions. If we assume $r_o = 0.3"$, $y_1 = 0.05"$, M = 40, U = 32 volt, R = 0.096, and V = 335 volt, then the maximum potential at the point of entry is:

$$(U + V)\ y_1^2/r_o^2 = (32 + 335)\ 0.05^2/0.3^2 = 10 \text{ volt}$$

This means that ions which leave the source with an energy of 21 electron volt can be accelerated in the fringe field to 31 electron volts if they enter the field in the right phase. The effect is even larger at the exit aperture, since this opening is wider. The energy gain is larger for heavier masses which require a proportionally larger V for transmission. It has been observed that if the exit aperture is kept more positive than the ionization chamber a spectrum is still obtained, which indicates that the ions have gained energy in the z direction. These spectra are completely suppressed for low mass numbers where the energy gain is insufficient to overcome the retarding field. The peak heights for high mass numbers are only moderately reduced.

The experiments with the retarding field on the exit aperture have been performed primarily to suppress the general background for high pressure operation. Since no improvement was found it must be concluded that stray ions have bypassed the exit aperture.

SECTION III

ION DETECTION

The output current of the monopole mass spectrometer is too small to permit direct measurement, except for the largest peaks. In order to achieve high sensitivity and fast scanning speed it is mandatory to use an electron multiplier. A 16-dynode copper-beryllium multiplier, ITT model FW4036, has been used. The performance of this multiplier was quite satisfactory. The gain was originally above 10^7 and decreased slowly during one year of testing to about 10^6. The original gain could be restored by baking the multiplier for 1 hour in 10^{-3} torr of oxygen at about 300°C. The "dark current" was extremely low, only a few counts per minute.

The anode current was usually measured with a conventional linear electrometer, especially for the performance tests of the monopole filter where the peak shape was of prime interest. The wide dynamic range necessary for recording of a real mass spectrum requires either range switching or a logarithmic electrometer. For simplicity reasons the latter one has been chosen.

A. Logarithmic Electrometer (see Figure 18)

This electrometer consists of an operational amplifier AR4 which has a high gain (20,000) and a high input impedance (10^{11} ohm). The feedback consists of a 10^8 ohm resistor in parallel with a log diode (TRW Model PS5831). This diode has a dynamic range from 10^{-11} to 10^{-4} amp and an output voltage of 5 mV to 530 mV; ΔV is about 0.07 volt per decade.

The amplifier feedback is reduced by the factor 0.058 which is temperature dependent to compensate exactly for the negative temperature coefficient of the diode. For this purpose, the 2K thermistor has been incorporated which has a negative temperature coefficient of 4 percent per C°.

The current scale is given by

$$i = 58 \times 10^{-11} \times U + (10^{0.83 \times U} - 1) \times 10^{-11} \text{ amperes}$$

where U represents the output voltage.

If U is smaller than 1 volt, the second term is small compared to the first one and the scale is essentially linear. If U is larger than 4 volts, the first term is small compared to the second one and the scale is essentially logarithmic. The advantage of this scale is that it has enough

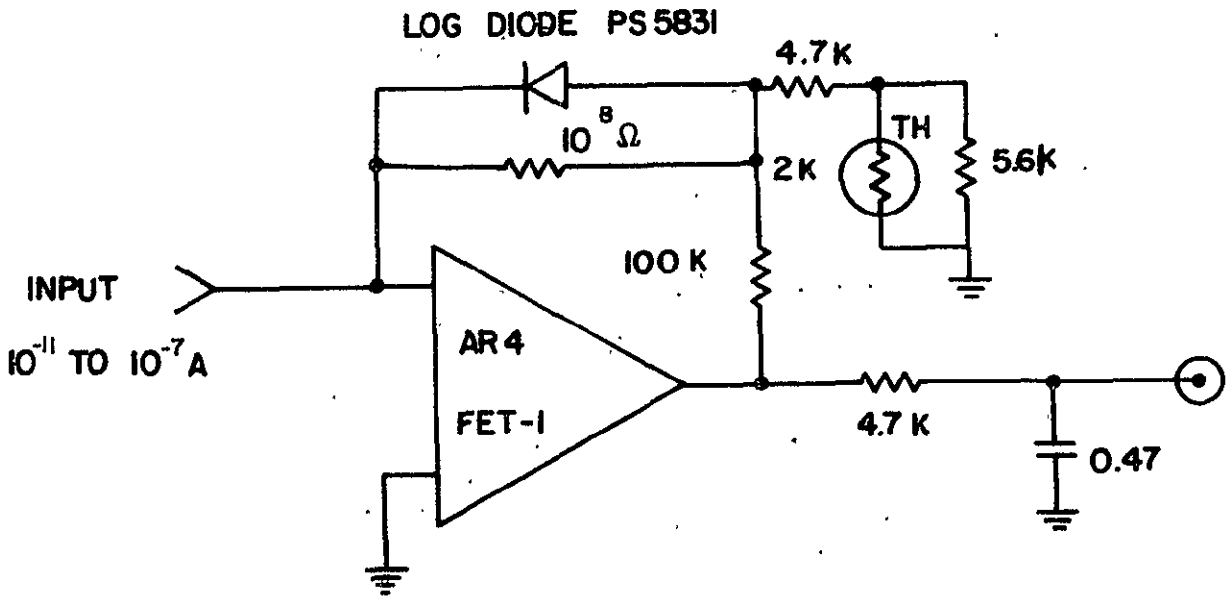

Figure 18. Log electrometer D ~~region~~ ~~spectrometer~~.

sensitivity to see even single ions with a time constant short enough to permit a fast scan. The middle part of the scale is expanded and permits a more accurate measurement of those peaks which are most likely expected. If there are occasionally very large peaks, they will stay on scale and can be measured on the compressed logarithmic part of the intensity scale.

Individual multiplier pulses are also readable in the electrometer output; in fact it was necessary to add an RC integrator to reduce their amplitude and the statistical noise present in a normal mass peak. The electrometer bandwidth is approximately 100 CPs and is determined essentially by the RC network.

B. Pulse Counting

Some preliminary experiments have been performed to test the advantages and limitations of pulse counting. The advantages are:

a. highest sensitivity
b. faster response than a high sensitivity electrometer
c. count rate almost independent of multiplier voltage
d. count rate almost independent of multiplier age

In order to realize these advantages it is necessary that the multiplier gain is at least 10^6, preferably 10^7 and that the threshold of the pulse amplifier is adjusted low enough to count almost all pulses. However, the threshold must still be high enough to prevent interference from external sources, TV and radio stations, transients in the power line, etc. and also from the RF power supply of the monopole itself. Shielding has to be performed with greatest care.

The conversion factor from ions to electrons on the first dynode depends mainly on the ion energy. About 10 keV would be required to obtain a 100 percent conversion. For practical reasons only 3.5 keV could be used which results in a conversion factor of about 30 percent which is about proportional to the voltage.

The background count rate, with the ion source switched off, is practically zero up to 3000 volt multiplier voltage and then increases linearly between 3000 and 3500 volt from zero to 2 counts per second. The count rate of a mass peak is about proportional to the multiplier voltage. Therefore, the best signal to noise ratio is obtained at about 3000 volt multiplier voltage.

The pulse amplifier is shown in Figure 19. The charge output from the multiplier caused by one single ion can be as small as about 2×10^{-14} coulomb

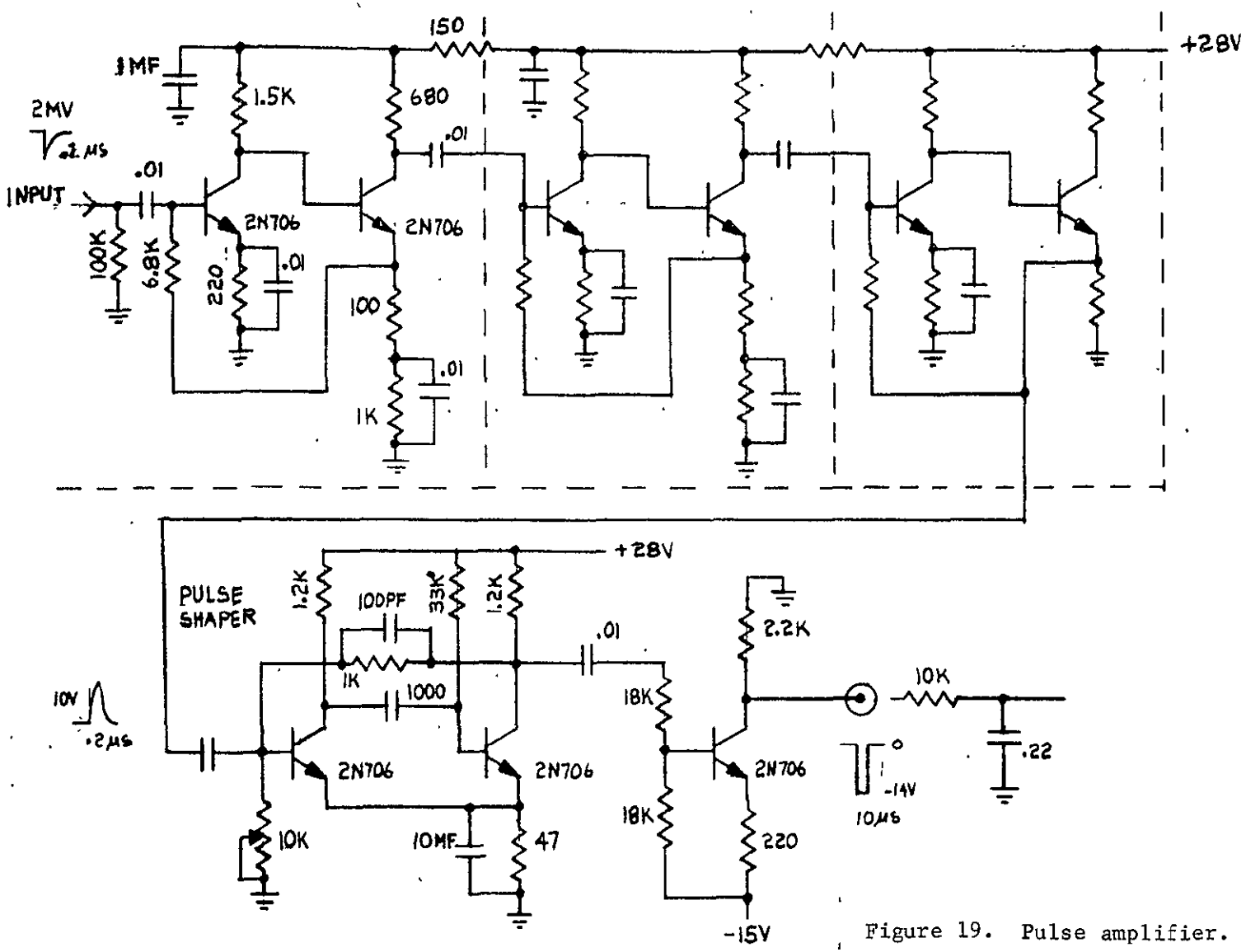

Figure 19. Pulse amplifier.

and has to be amplified by a wide bandwidth AC amplifier. In general, the pulse width has to be maintained narrow to prevent loss of accuracy due to pulse overlap. This loss of accuracy is negligible except for the largest peaks. A pulse amplifier was constructed using 3 double and one single shot multivibrator as a pulse standardizer.

The multiplier output at the input of the pulse amplifier was measured to be about 2 mV peak height and 0.1 μs width. The pulse amplifier output driving the monostable multivibrator is a 10 V peak, 0.2 μs wide. The monostable multivibrator and the output driver were adjusted to deliver a standardized 10 μs wide pulse with 14 volt amplitude into the 10 k and .22 MF RC integrator. RC was chosen to produce a peak amplitude of 100 mV for a single input pulse. This value is easily detectable on the recorder chart.

Experimental results indicate that the integrator output is approximately a logarithmic function of the count rate. Saturation occurs if the pulse rate exceeds 2×10^5 counts/sec. In this case, the output voltage is -14 volt The relatively long duration of the output pulses (10μs) has been chosen for the particular application as a D-region ion spectrometer. It is expected that the maximum count rate stays well below the 2×10^5 counts/sec limit. However, the sensitivity is high enough to see even a single ion.

The counting technique has been used successfully to test the performance of the monopole mass spectrometer for negative ions. Figure 20 shows the potentials applied to the electron multiplier and the capacitive coupling to the pulse amplifier. In this case, the anode is at 4 kV above ground which prohibits the use of a normal electrometer. The isolation capacitor has to be of the highest quality to prevent corone discharges which would increase the background counts. A ceramic transmitting capacitor from Centralab Model 8585 100 pF, 5000 VDCW performed satisfactorily. A typical spectrum of negative ions, obtained with the pulse counting technique, is shown in Figure 17.

C. Peak Integrating Technique

The total number of ions within one mass peak is considerably larger than the number of ions counted during the very short time interval of maximum peak intensity. Therefore, the accuracy of a measurement of the peak integral is much better than that of the maximum peak height. This is especially true for very small peaks and for fast scans with high resolution. If the entire peak consists of only a few ions it becomes unlikely that even only one ion arrives exactly in the center of the peak. Therefore, the maximum peak height is no longer a measure of the ion current which is better represented by the total number of ions within one peak. This method of

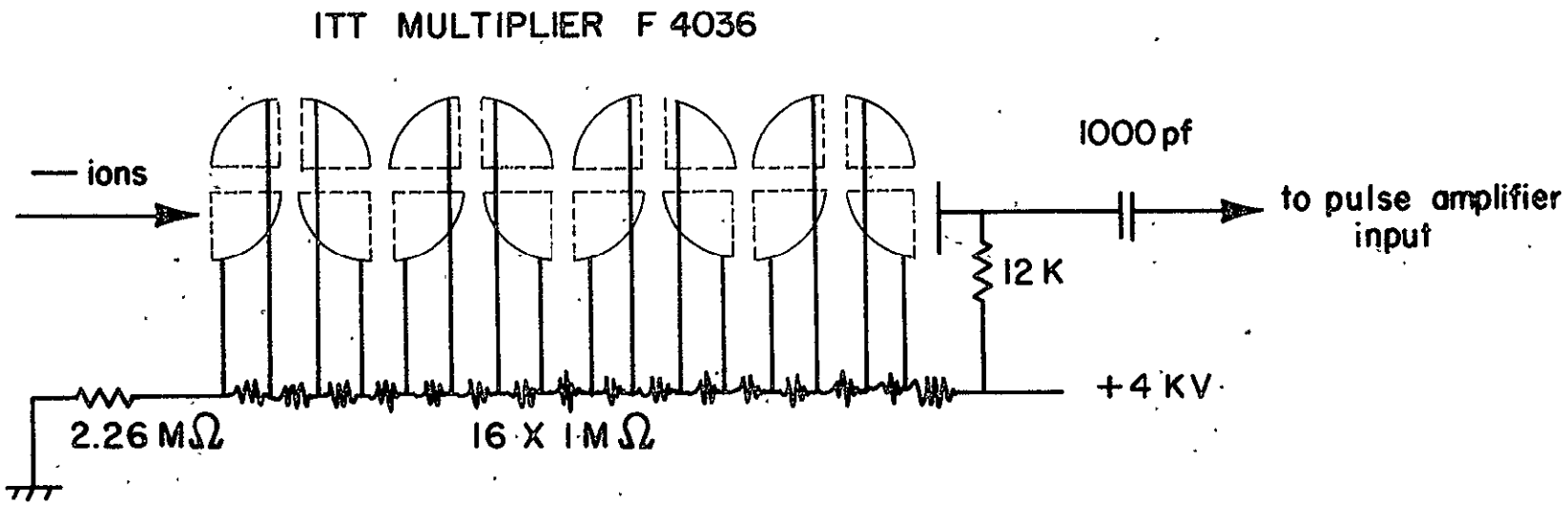

Figure 20. Multiplier connections for negative ion counting.

evaluation of a mass spectrum is greatly simplified by the fact that the spectrum of a monopole mass spectrometer consists of peaks of equal width and that a linear mass scale can be easily achieved. Application of this method would be easy if the spectrum would consist only of peaks of approximately equal height. Unfortunately, this is not the case. If a linear scale is used, the output is either overdriven by the larger peaks or the small peaks are lost. For the D-region mass spectrometer the detection of all peaks, including the smallest ones is more important than the accurate measurement of the peak heights. This can be done with the integrator circuit shown in Figure 21. The pulse width has been enlarged to 3 m sec which results in saturation at about 600 ions per second. Therefore, the large peaks are clipped to permit detection of the small peaks. Figure 22 shows an air spectrum which was obtained by this method. The height of the steps is related to the peak heights and has to be calibrated individually. The telemetry of this staircase function is much simpler than the telemetry of a regular mass spectrum which consists of sharp and narrow peaks. Therefore, this method will have an advantage for deep space probes where the telemetry capability is rather limited.

Unfortunately, work on the pulse counting technique had to be stopped because it was not an explicit contract requirement and time and funds were not available to incorporate this method into the flight hardware. The contract monitor decided to use the logarithmic electrometer for the flight model.

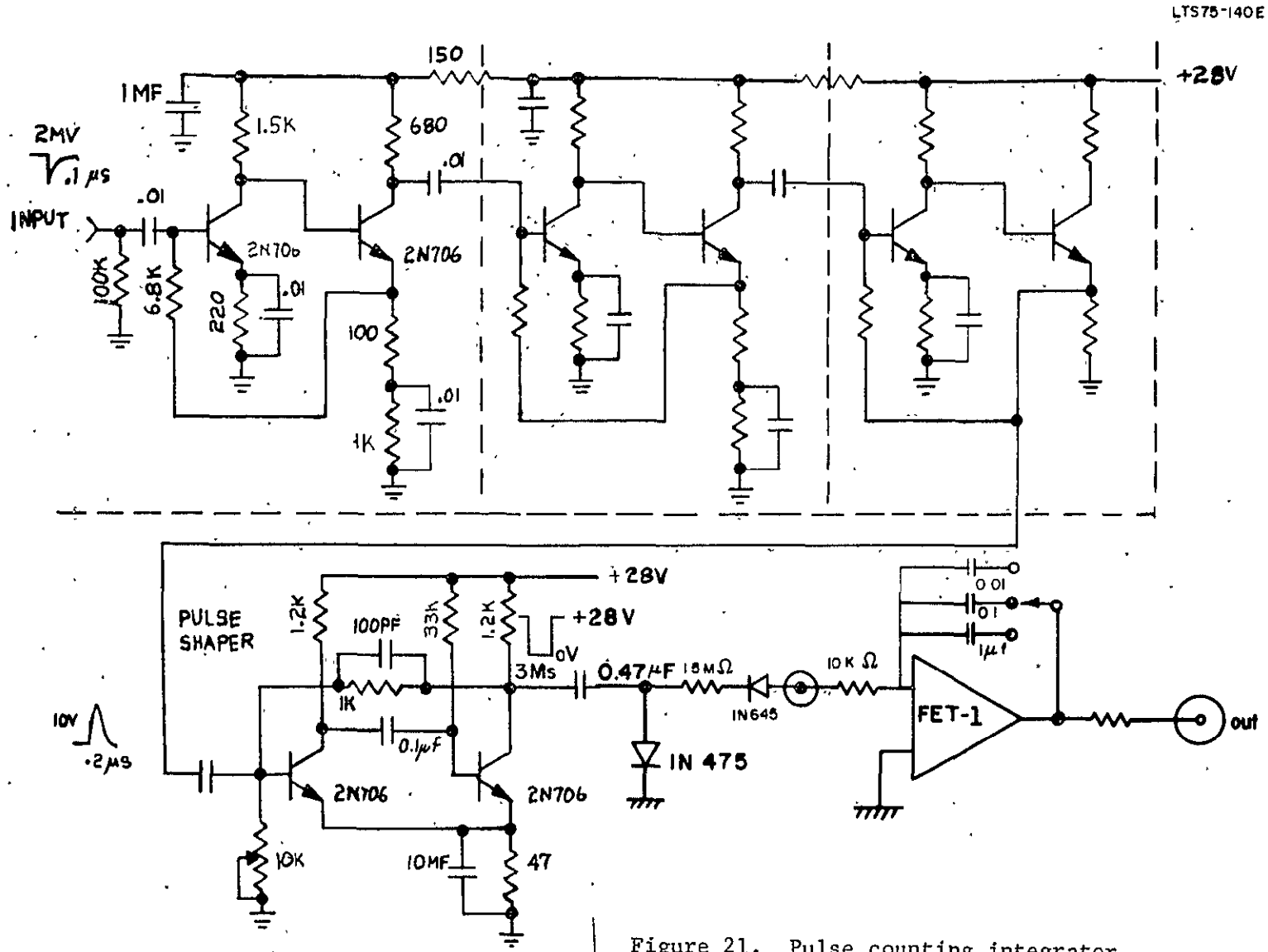

Figure 21. Pulse counting integrator.

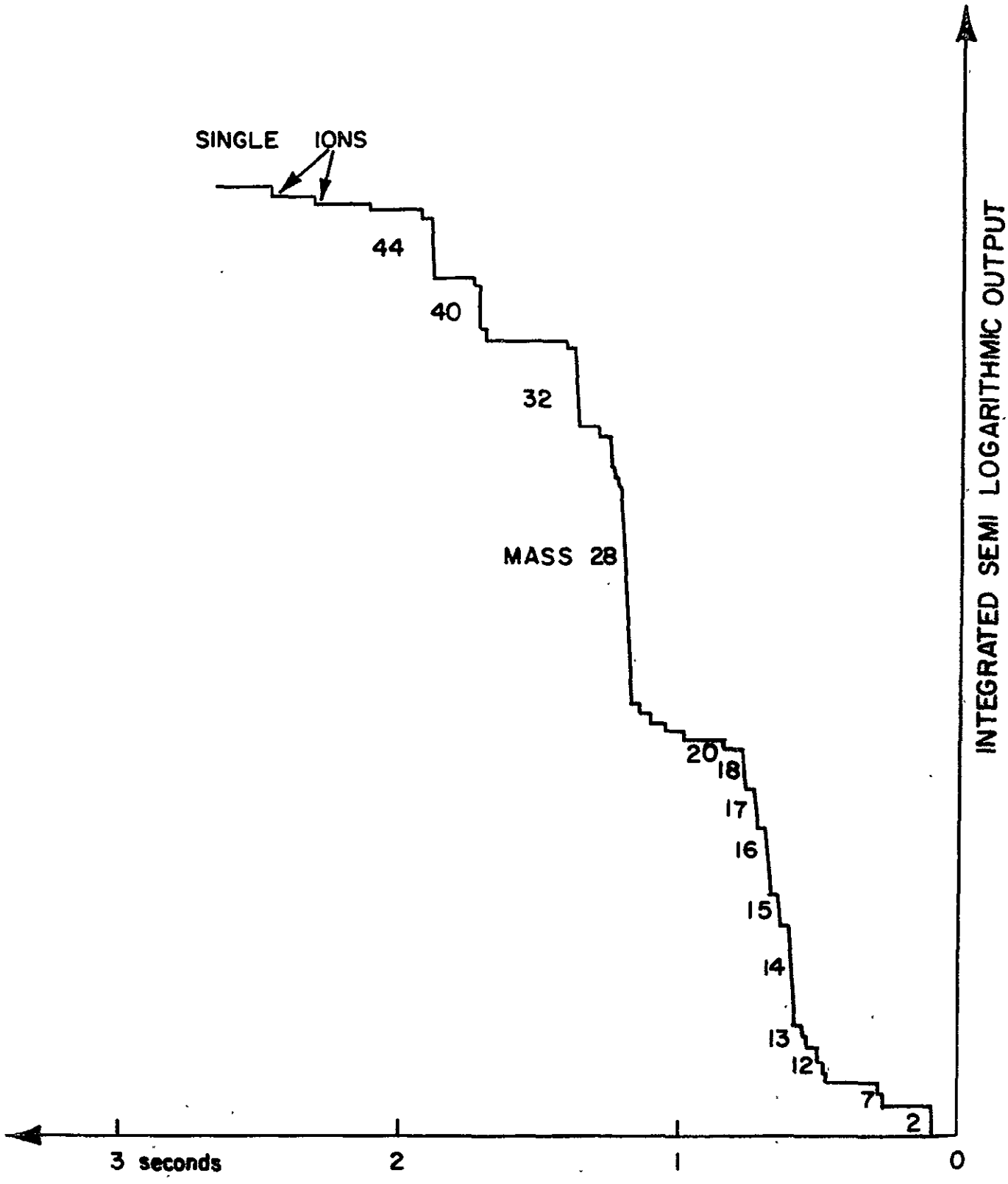

Figure 22. Integrated mass spectrum of air, p = 2 x 10^{-8} torr. (Positive ions).

SECTION IV

TITANIUM GETTER PUMP

The pressure in the D-region of the atmosphere is too high to permit operation of the mass spectrometer without differential pumping. Bailey and Narcissi (Ref. 13) have used Zeolite absorption pumps for this purpose. Such a pump has to be cooled with liquid nitrogen before the launching of the rocket. Condensation of water near the filling tube for the liquid nitrogen and evaporation of this deposit during flight may be responsible for contamination of the environment with water vapor. Another disadvantage of these pumps is the relatively slow diffusion of the gas into the Zeolite. If suddenly a large amount of gas is introduced into the system the pressure will first rise suddenly and then decrease slowly until most of the introduced gas is absorbed. A titanium getter pump is free from these drawbacks, and has therefore been incorporated into the mass spectrometer system. In ordinary titanium getter pumps the titanium film on the wall is continuously or intermittently renewed by evaporation of fresh titanium. This approach is not well suited for rocket application because the power consumption is too high. Therefore, it was decided to produce the titanium getter film before the rocket launch and to determine experimentally the absorption capability of such a titanium layer. It was found experimentally that the method of preparation of this layer has a great effect on the total absorption capability. If the titanium film is produced at medium vacuum by evaporation of a titanium filament then the absorption capability is rather poor. During the evaporation process a very large amount of hydrogen and CH_4 is released and these gases occupy a large number of absorption sites of the evaporated titanium film. A much higher absorption capacity was found if the film was produced under ultra high vacuum conditions. The simplest way to achieve this is by means of an orb ion pump.

A. Orb Ion Pump

Such a pump consists of an electrode arrangement which electrostatically confines a dense electron cloud. This electrostatic confinement has been investigated by Herb (Ref. 14). Pump constructions have been described by Herb et al (Ref. 15) and by Maliakal, et al (Ref. 16). The field is produced by a thin wire which is kept at a high positive potential and a surrounding concentric tube with two end plates which are kept at ground potential. Electrons are emitted from a hot filament which is kept at a slightly positive potential against ground which prohibits electrons from reaching the inner wall of the cylinder or the end plates. A shield between the filament and the anode prevents electrons from falling directly from the filament to the anode. All electrons are ejected in different directions and their trajectories are open loops around the anode oscillating back and forth along

the cylinder. Therefore, a very dense electron cloud will accumulate and ionize the gas by electron impact. The positive ions are pushed toward the outer wall of the pump. Electrons are retarded during the ionization process and will finally fall on the anode. The anode consists of a thin tungsten or molybdenum wire which carries a titanium cylinder in the center. This titanium is heated by the impact of the electrons and starts to evaporate if the total power dissipation is sufficiently high. The evaporated titanium condenses on the walls of the pump and reacts with the ions which are impinging there. Active gases like oxygen, nitrogen and hydrogen are chemically bound to titanium. The rare gases are physically absorbed and finally buried under new layers of titanium.

The initial experiments have been performed with a 6" Orb Ion Pump manufactured by NRC. The general performance of this pump was quite satisfactory. The starting of the pump is sometimes difficult since it requires a pressure of 10^{-4} torr or less and since initially large amounts of gas are released from the titanium anode. After the pump was previously in operation and is fairly well outgassed the starting is much easier. The starting vacuum was provided by a liquid nitrogen cooled Zeolite pump. The electron emission of the Orb Ion Pump has to be increased quite slowly because of the large initial outgassing and the requirement to keep the pressure in the pump below 10^{-4} torr. It may take several hours until the normal operating conditions of 10 kV and 50 MA are reached. About 40 MA are enough to start the evaporation of titanium. If this occurs the pressure drops rapidly and within a few minutes it is in the 10^{-7} range. Further decrease is slow and after about a day of pumping the 10^{-9} range will be reached. The lowest pressure obtained was about 2×10^{-10} torr after a thorough bake-out of the whole system at 400°C for about 12 hours.

Measurement of the pumping speed with oxygen, nitrogen and argon have bee performed and confirm essentially the specifications of NRC. Pumping speed measurements are difficult to perform since equilibrium conditions are obtaine very slowly. If the titanium layer on the wall is thin and new, the pumping is performed essentially only by the newly deposited titanium and therefore dependent on the evaporation rate which is a function of the electron current. However, if a thick and active titanium layer has been previously deposited on the walls most of the pumping is performed by this layer and the evaporation rate is not very critical. If a large amount of gas is introduced suddenly into the pump it will be absorbed readily if the pump has been in operation a long time. However, it will cause instability and stop the operation of the pump if there is not a sufficient amount of titanium on the walls. The pumping speed for other gases has not been measured explicitly, but it appears that hydrocarbons and fluorocarbons are removed quite readily. Water vapor was removed extremely slowly and if introduced in somewhat larger quantities it resulted in complete break-down of the pumping operation.

Therefore, it is quite worthwhile to thoroughly dry all gases which are introduced into the system. Especially if the system is vented to atmospheric pressure it should be done with dry nitrogen. Even with this precaution, the background spectrum of the unbaked system shows a predominant water peak. If the system is well baked the water peak becomes rather small and the largest peaks in the spectrum are CO and CO_2. If a new titanium rod has been installed a large amount of CH_4 is released. However, this gas becomes unimportant after the pump has been in operation for a few days. The H_2 peak depends on the temperature of the pump wall. If the wall is hot, as during the bake-out operation, the H_2 peak is by far the largest peak of the background spectrum and is caused by thermal decomposition of titanium hydride. However, if the pump wall is water cooled, the H_2 peak becomes rather small since the Orb Ion Pump has a high pumping speed for hydrogen.

If the well baked pump is switched off a rather large amount of superfically buried argon is released whereas other background gases such as hydrogen, CO, and CO_2 are reduced probably because the main source of contamination, the titanium rod, has cooled down. As a result, the background gas of the switched off pump consists practically of pure argon. Many performance tests of the monopole mass spectrometer have been made with the pump switched off, since in this way very constant and reproducible operating conditions have been achieved.

Occasionally the Orb Ion Pump produced intense high frequency oscillations which were extremely disturbing for other equipment. The frequency was in the 10-100 MHz range and the large intensity was pulsating at very low frequency. Shielding of the cables and a damping resistor in the anode line had little effect on the disturbance. However, a small positive bias potential on the filament completely suppressed the plasma oscillations. The adjustment of this bias potential is critical since the regions with suppress oscillations alternate with regions of strong oscillations if the bias voltage is steadily increased. Approximately 30 V were sufficient to suppress the oscillations.

The 6" pump is too large and too heavy for any flight application. Therefore a smaller model has been built which is shown in Figure 23. Approximately 8 kV and 17 MA were adequate to start evaporation of the titanium rod. Air cooling of the housing was sufficient since the power consumption of this pump in normal operating conditions is only approximately 140 W. The performance of this small pump was quite satisfactory and the pumping speed was limited only by the inlet tubulation to approximately 40 liters/sec if the pressure was below 10^{-6} torr. At higher pressure the pumping speed is reduced or the current has to be increased.

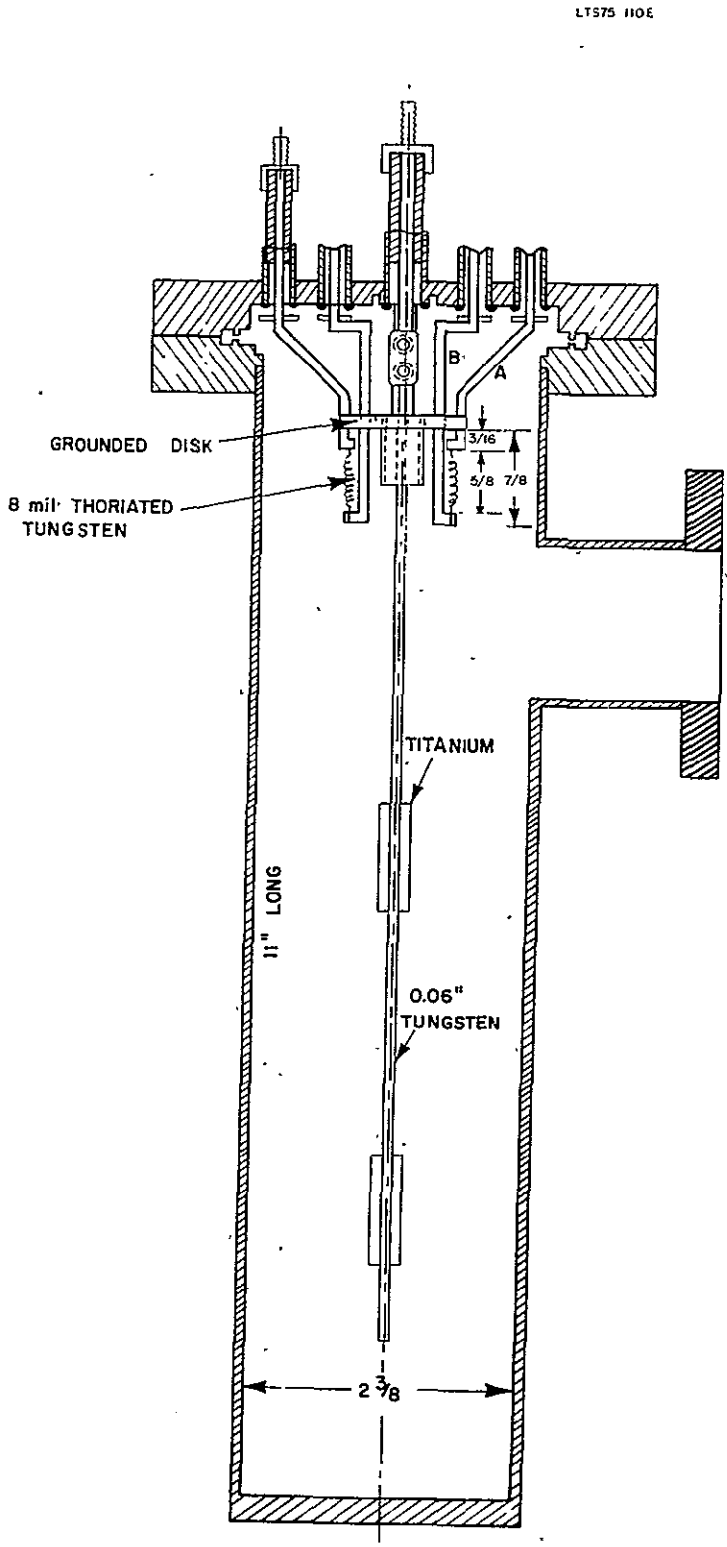

Figure 23. Small orb ion pump.

A comparison between sputter ion pumps and the Orb Ion Pump turns out in favor of the Orb Ion Pump, especially for space applications, since these pumps can be made much lighter because no permanent magnet is needed. Since in the Orb Ion Pump the fresh titanium is removed from the anode by evaporation no instability for argon can occur. The power consumption of the Orb Ion Pump is higher than the power consumption of a sputter ion pump of the same pumping speed if the Orb Ion Pump is operated in such a manner that the titanium evaporates. For many applications where a limited gas load has to be pumped, this is not necessary. If a heavy and well activated titanium layer has been deposited on the walls then a very small electron current of approximately 1 MA is enough to provide ionization of the gas and good pumping for all gases including argon. The power consumption under these conditions is only a few watt and no external cooling is necessary. The fact that no magnetic field is needed to operate this pump is extremely valuable for space applications if instruments which are sensitive to magnetic fields are on the same vehicle. A sputter ion pump has to be shielded very carefully which will further increase the weight of such a pump.

Ruggedization of the Orb Ion Pump to make it useful for space applications is an intriguing material problem. The anode of the pump is a tungsten wire of 60 mil diameter with a small titanium cylinder in the center. During operation this wire becomes extremely hot and recrystallizes. Thereafter it is very brittle and the pump has to be handled carefully. Support of the wire at the other end provided some improvement but still not enough to guaranty survival of the anode structure during rocket launch. Experiments with a tungsten cable, which was quite flexible before installation, were not successful. Apparently the molten titanium reacted with the tungsten and the alloy became extremely brittle. Further work will be necessary to overcome this difficulty.

B. Titanium Getter Pump

For the application in the D-region mass spectrometer is was planned to use only the getter action of a newly evaporated and activated titanium layer on the wall of the pump. The inner structure of the Orb Ion Pump is only used to produce this active titanium layer before launch of the rocket. No voltages are applied to the pump during the actual flight. Therefore it is immaterial whether or not the anode structure breaks during the launch.

A large number of experiments have been performed to study the absorption capabilities of the titanium layer. For this purpose a small volume of 1.2 cm^3 was filled with air of known pressure, usually a few torr. This volume of air was released into the pump after a titanium layer had been deposited on the wall and the pump had been switched off. The change of the partial pressure of the main components of air has been observed and recorded with the monopole mass spectrometer. The following results have been observed.

Argon.- As expected, this gas is not absorbed at all. The partial pressure increases in proportion to the total amount of gas introduced and stays perfectly constant thereafter. Since approximately 1 percent of the introduced air is argon this effect limits the total amount of air which can be introduced into the system without exceeding a given pressure. The total volume of the monopole mass spectrometer with the getter pump is 1800 cc and the maximum operating pressure for the monopole mass spectrometer is about 8×10^{-4} torr. The total amount of argon in the system is 1.44 torr cm^3. This means that 144 torr cm^3 of air can be introduced into the system if all the other gases were completely removed by absorption. Unfortunately, this is not the case since nitrogen is not completely absorbed.

Oxygen.- This gas is pumped extremely rapidly and completely. Even after very large quantities of air have been admitted the oxygen peak disappeared completely after a few seconds.

Nitrogen.- Since this is the main constituent of the lower atmosphere the absorption characteristic for nitrogen is extremely important. If the pump wall is at room temperature the absorption of nitrogen is slower than of oxygen and less complete. If successive samples of air are introduced each following sample is absorbed more slowly and a higher residual background pressure of nitrogen remains. After the introduction of 26 torr cm^3 of air a total pressure of 4.7×10^{-3} torr was observed. If all but the rare gases had been completely absorbed, the pressure should have been 0.15×10^{-3} torr. This indicates that the titanium layer was practically saturated.

In order to study the absorption capability of a saturated titanium layer this gas was removed with the large Orb Ion Pump until the pressure in the system was again in the 10^{-8} range. Then the valve between the pumps was closed and an equilibrium pressure of 5.7×10^{-7} torr was finally reached in the small ion pump. A small amount of air (0.84 torr cm^3) was introduced into the pump. There was still some absorption capability left in the titanium layer. However, it took 3 minutes to reduce the nitrogen partial pressure by one order of magnitude. A following very small sample of 0.18 torr cm^3 was only half absorbed. After 4 minutes the height of the 28 peak became constant indicating that the titanium layer was now completely saturated. Heating of the wall of the pump was then started. It was expected that outgassing would occur and the pressure would rise. The opposite happened. At about 140°C the pressure started to fall and at 275°C the partial pressure of nitrogen was practically zero. Under these conditions 6 more large samples of air, each 1.8 torr cm^3, were introduced and saturation was still not reached. The total pressure was only 5×10^{-5} torr and the background gas consisted mainly of argon (92 percent) and nitrogen (7 percent). Trace amounts of He, Ne, Kr, and Xe and also H_2, CH_4, H_2O and CO_4 were also visible (see Figure 24).

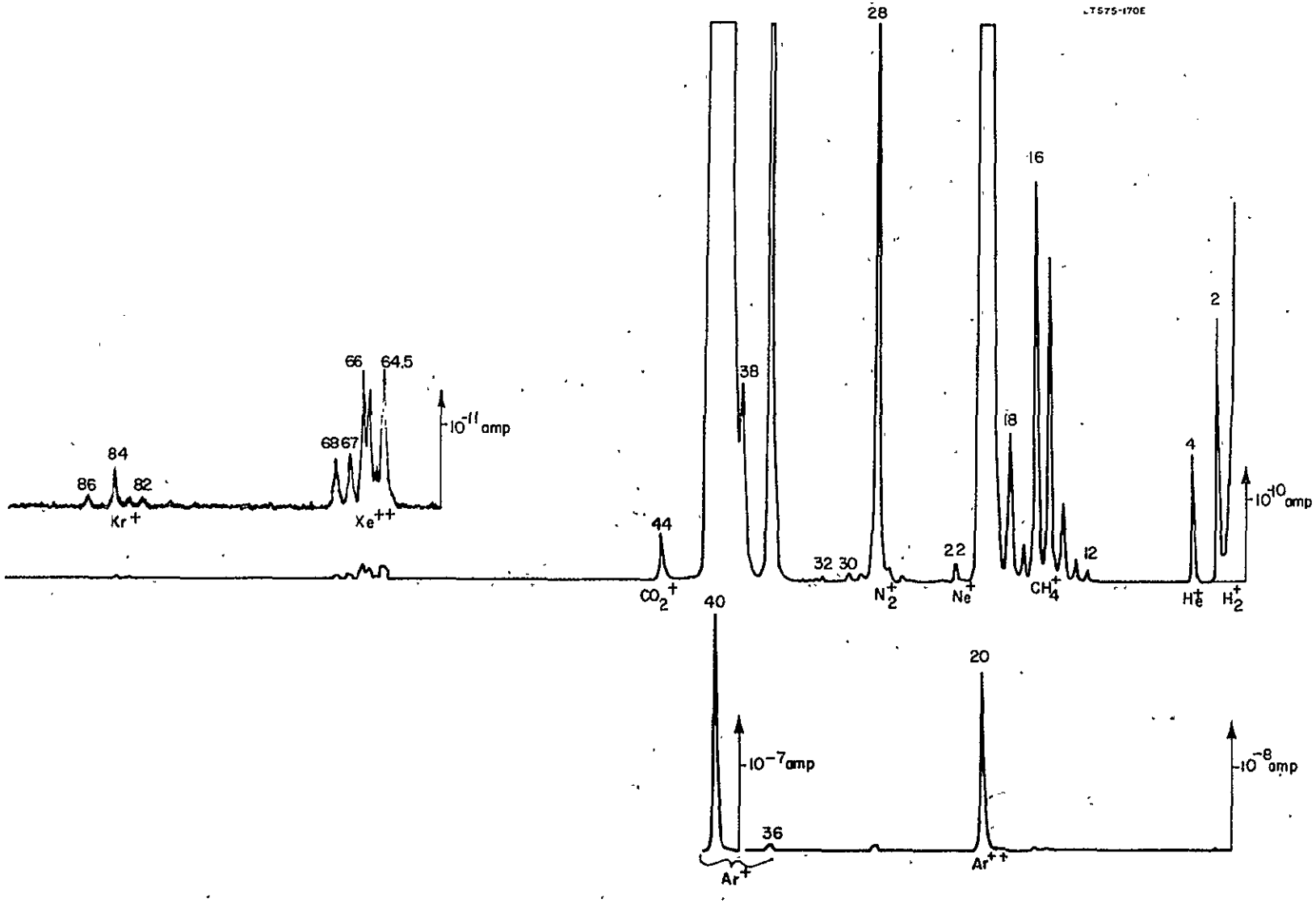

Figure 24. Restgas analysis after absorption of a large amount of air.

Water vapor.- The fresh titanium layer did absorb water vapor but rather slowly. The partial pressure dropped one order of magnitude in about 3 minutes. This result was surprising since the Orb Ion Pump was quite ineffective in removing water vapor. Actually it was observed that in a closed system the partial pressure of water vapor did rise considerably when the Orb Ion Pump was switched on.

C. Calculation of the Expected Operating Range and Sensitivity

For the purpose of this rough calculation we assume that the mass analyzer will be installed in the nose cone of a Nike-Cajun rocket which, under the given load conditions, will reach a top altitude of 110 km. The intake aperture is assumed to be in the forward direction in order to be insensitive to small angles of attack. Table 4 below shows the rocket velocity, v, the ambient pressure, P, and the stagnation pressure, P* as a function of altitude, h. T is the ambient temperature and T* the temperature of the compressed gas behind the shock wave in front of the entrance aperture.

TABLE 4

STAGNATION PRESSURE AND TEMPERATURE

h km	v_{rocket} km/sec	P microns	P* microns	^{o}T ^{o}K	$^{o}T^*$ ^{o}K
60	1.00	190	2300	253	518
65	0.95	96	1170	231	472
70	.90	45	550	210	430
75	.85	19	230	187	382
80	.78	7.5	88	165	338
85	.71	2.8	27	165	314
90	.63	1.0	7.9	165	300
95	.55	0.4	2.3	178	296
100	.45	0.2	0.6	199	300

This table shows that the stagnation or ram pressure is about one order of magnitude above the ambient pressure which puts a heavy load on the pumping system.

The number of molecules passing per second an orifice of area A cm^2 is given by:

$$\nu = 6.5 \times 10^{18} \frac{A \cdot P^*}{\sqrt{T^*}} \tag{73}$$

where P* is measured in microns. The total number of molecules, N, which enter the mass spectrometer in the time interval from t_1 to t_2 or in the corresponding altitude interval from h_1 to h_2 is given by

$$N_{h_1}^{h_2} = \int_{t_1}^{t_2} \nu dt = 6.5 \times 10^{18} \times A \times \int_{h_1}^{h_2} \frac{P^*}{\sqrt{T^*}} \quad \frac{dh}{v_{rocket}} \tag{74}$$

This integral is mainly a function of h_1, the lowest altitude where the instrument is opened during ascent of the rocket. The upper altitude h_2 has very little effect as long as it is near the peak of the trajectory.

Evaluation of this integral for the parameters listed in Table 4 results in the N/A values listed in Table 5:

TABLE 5

MAXIMUM PERMISSIBLE SAMPLING ORIFICE

h_1	N/A	A	D
58 km	$6.8 \times 10^{21}/cm^2$	0.00015 cm^2	0.14 mm
63	3.5	0.0003	0.20
68	1.7	0.0006	0.28
73	0.73	0.0014	0.37
78	0.29	0.0035	0.67
83	0.10	0.01	1.1
88	0.03	0.03	2

The experiments with the small titanium getter pump have shown that an active titanium surface of about 150 cm^2 is capable of absorbing 15 micron liters of air or 5×10^{17} molecules until the nitrogen partial pressure rises to about 1×10^{-4} torr corresponding to the formation of about 4 monolayers. This is not the limit of the absorption capability for nitrogen. However, further absorption proceeds slower unless the pump walls are heated to about 200°C. In this case about 3 times as much nitrogen can be absorbed.

The argon partial pressure can be calculated by simple expansion into the total volume of the system.

The size of the pump, which can be used for the proposed instrument, is limited by the space available in the rocket. An activated wall of 300 cm^2 seems to be reasonable, corresponding to a total pumping capacity of 10^{18} molecules. If we assume a total system volume of 5 liters then the argon partial pressure will rise to 6×10^{-5} torr which is quite tolerable. Based on these figures, the maximum allowable entrance aperture can be obtained from Table 5; A is the area and D the diameter of the entrance aperture. As expected, the entrance aperture must be reduced if the mass spectrometer is opened at a lower altitude.

The next step is to calculate the ion current that enters the instrument. Let us assume an entrance aperture of D = 0.37 mm. The number of neutral particles ν_o entering the instrument per second is given by Equation (73) and computed in Table 6:

TABLE 6

AMBIENT GAS INTAKE

h	ν_o	ambient particle number density	volume flow
60 km	940×10^{15} sec^{-1}	7.3×10^{15} cm^{-3}	132 cm^3/sec
65	500	4.0	122
70	240	2.1	112
75	110	1.0	104
80	43	0.44	94
85	14	0.16	85
90	4.3	0.06	75
95	1.3	0.02	66
100	0.4	0.008	47

The ratio of ν_o to the ambient neutral particle number density is the volume flow expressed in cm^3/sec at the corresponding ambient pressure. It can be seen from Table 6 that the volume flow does not vary much over the altitude range considered. The decrease at higher altitudes is due to the reduced rocket velocity and to the lower ambient temperature. We may assume an average volume flow of about 100 cm^3/sec for the chosen aperture. The maximum ion density in the D-region is about 10^4 ions/cm^3 which corresponds to a total ion current of 10^6 ions/sec entering the mass filter. These ions enter the instrument from all directions and, even after being collimated by the accelerating field and lens system, only a fraction of these ions are able to pass the filter. A conservative estimate, based on previous experimental results, indicates that about one percent transmission can be achieved. Based on the figures mentioned above, we can expect that an ambient ion density of 10^4 ions per cm^3 will produce a collector current of 10^4 particles per second. The measurement of these small currents is basically limited by the statistical nature of the ion current. A fair accuracy can only be achieved if the longest possible integrating time is used. About 1/10 second per mass peak seems to be a reasonable figure compatible with the rocket speed and the expected change of ambient ion density. Under these conditions, the practical detection limit is about 10 particles per second or 10 ions per cm^3.

The sensitivity can be considerably increased if the measurements are started at higher altitudes. It can be seen from Table 5 that the entrance aperture A can be increased by a factor of 10 if the altitude where the instrument is opened is increased from 73 to 85 km. Under these conditions the sensitivity and the detection limit will be increased by one order of magnitude. The sensitivity can be significantly increased or the instrument opened at lower altitude if the pump walls are kept at about 200°C during the short flight time of the instrument, which can be easily done. However, the most important improvement would be to operate the pump, even if the electron current is as low as 1 ma.

Based on the results obtained with the laboratory model described in this report a flight prototype was designed, built and tested. This work is described in detail in the second part of this final report which was submitted earlier.

REFERENCES

1. Zahn,Ulf von, Rev. Scient. Instr. 34, 1, 1963.

2. Lever, R. F., IBM Journal, p. 26, 1966.

3. Dawson, P. H., and N. R. Whetten, Rev. Scient. Instr. 39, 1417, 1968.

4. Brubaker, W. M., USAF Contract No. AF 19(604)-5911, Quarterly Reports 20 June and 13 September 1960.

5. Herzog, R. F., Rev. Scient. Instr 40, 1104, 1969.

6. Brubaker, W. M., Recent Developments in Mass Spectroscopy, ed. by Ogata and Hayakawa, University of Tokyo Press, p. 98, 1970.

7. McLachlan, Theorie and Applications of Mathieu Functions, Oxford University Press, London, p. 133, 1951.

8. Herzog, R. F., The Monopole Mass Spectrometer and its Advantages for Upper Atmosphere Research, Aeronomic Conference, University of Illinois, 21 October 1963.

9. Grande, R. E., R. L. Watters, and J. B. Hudson, J. Vac. Sci. Tech. 3, 329, 1966.

10. Herzog, R. F., J. Vac. Sci. Tech. 6, 955, 1969.

11. Herzog, R. F., 15th Conference Mass Spectr., Denver, p. 549, 1967.

12. Paul, W. and H. Steinwedel, Z. f. Naturf. 8a, 448, 1953.

13. Bailey, A. D. and R. S. Narcisi, AFCRL-66-148, February 1966. Instrumentation Papers, No. 95.

14. Herb, R. G., Rev. Scient. Instr. 35, 569, 1964.

15. Herb, R. G., T. Panly, R. D. Welton and K. J. Fisher, Rev. Scient. Instr. 35, 573, 1964.

16. Maliakal, J. C., P. J. Limon, E. E. Arden and R. G. Herb, J. Vac. Sci. Techn. 1, 54, 1964.